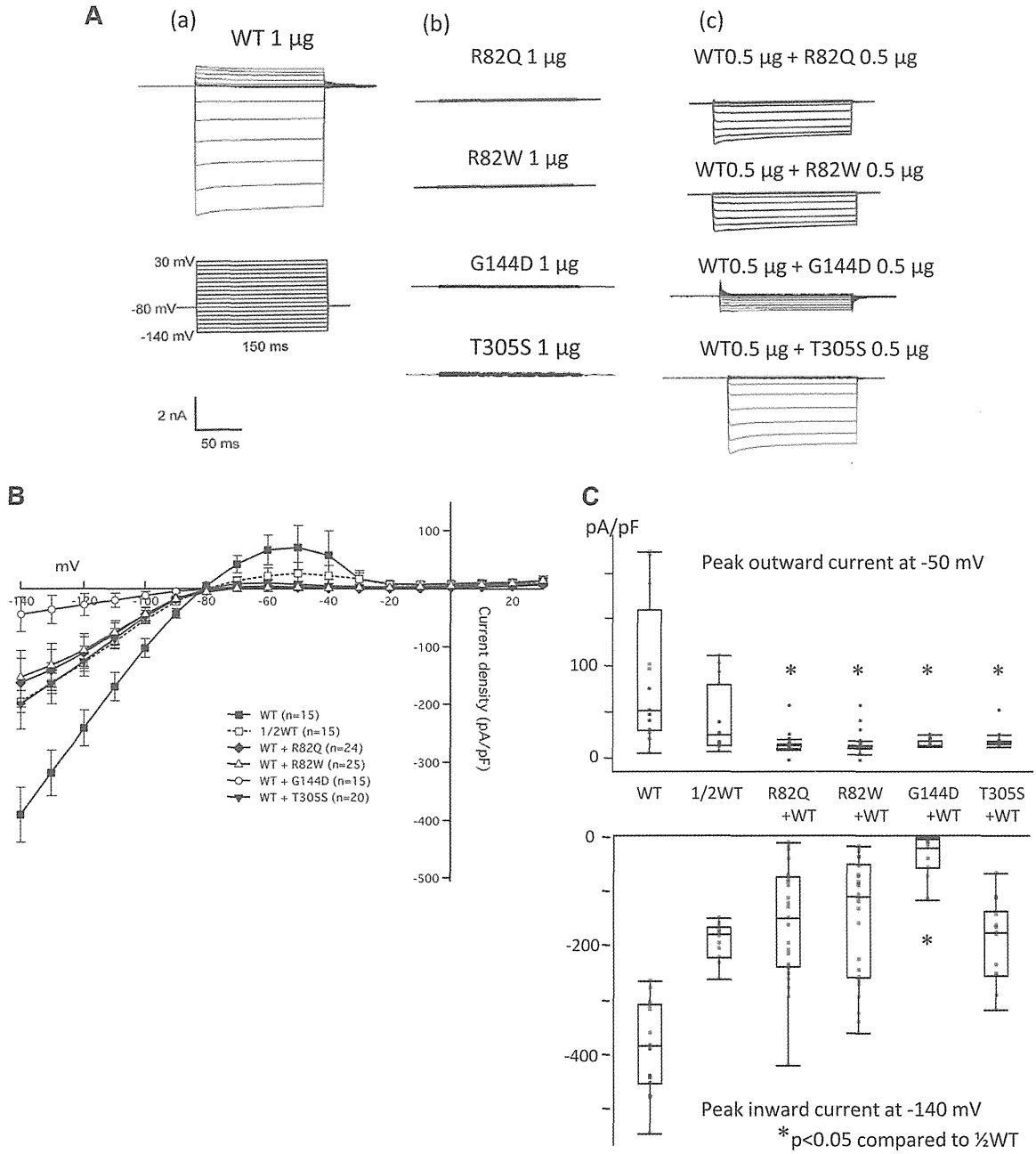


**Figure 4.** Functional analyses of mutated Kir2.1 channels found in group B. **A**, Representative Kir2.1 currents expressed in CHO cells: **a**, wild-type (WT) cDNA 1 μg; **b**, R82Q (1 μg), R82W (1 μg), G144D (1 μg), and T305S (1 μg). Cells were held at −80 mV. **c**, Cotransfection with WT (0.5 μg) and each mutant, R82Q (0.5 μg), R82W (0.5 μg), G144D (0.5 μg), and T305S (0.5 μg). Square pulses of 150-ms duration were applied to the potentials between −140 and +30 mV with 10-mV increments. Scale bars indicate 50 ms and 2 nA. **B**, Plots for current-voltage relationships obtained by multiple experiments of the same protocol as shown in **A**. Current densities were calculated by dividing with cell capacitance. **C**, Dot plots showing mean current densities in WT (1 μg, n=15), 1/2WT (0.5 μg, n=15), cotransfection with WT (0.5 μg) and R82Q (0.5 μg) (n=24), WT (0.5 μg) and R82W (0.5 μg) (n=25), WT (0.5 μg) and G144D (0.5 μg) (n=15), and WT (0.5 μg) and T305S (0.5 μg) (n=20). **Upper panel**, Those at −140 mV; **lower panel**, those at −50 mV.

waves. Accordingly, probands in this group received a genetic diagnosis at a significantly older age. Among the 3 features of ATS, dysmorphic features could be seen from the infant period; in contrast, ventricular arrhythmia appeared later, presumably because the $I_{K1}$ current could be reduced in females by gonadal steroids.[29] The ATS-related phenotype was reported to be dependent on sex[30]—female subjects with *KCNJ2* R67W from a white family displayed ventricular

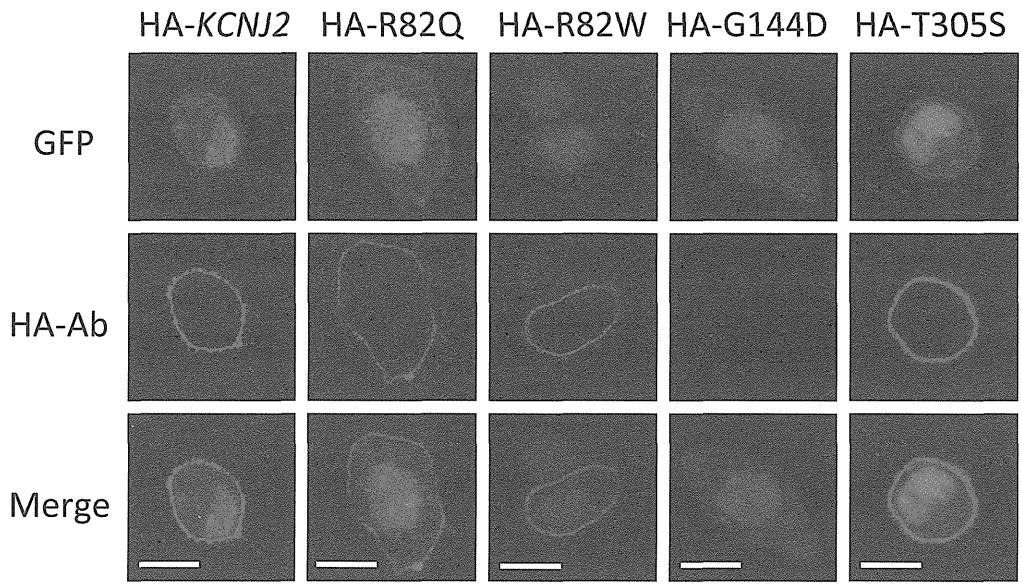


**Figure 5.** Cellular localization of wild-type (WT) and 4 mutant (R82Q, R82W, G144D, T305S) Kir2.1 channels. Hemagglutinin (HA)-*KCNJ2* indicates HA-tagged *KCNJ2* (positive control). **Upper panel** shows the green fluorescence of GFP; **middle panel**, red fluorescence of secondary anti-HA antibody; **lower panel**, merging of green and red fluorescences; **white bars** in the **merged panel** indicate 10 $\mu$m.

arrhythmias after the age of 10 years, and arrhythmias were reduced during pregnancy and after age 55 years, coinciding with menopause. In contrast, male mutation-positive subjects from the same family showed no ventricular arrhythmias but periodic paralysis. Interestingly, a case with R67W in our cohort was a male and complained of only periodic paralysis, supporting their conclusion, although there is a conflicting report by Donaldson et al.[26] They reported that the R67W mutation is capable of causing all phenotypes of ATS, and the pattern observed in the sex-specific kindred is not universal. It appears that other genetic or environmental factors contribute to a family's susceptibility to disease symptoms.

The topological location of *KCNJ2* mutations may influence the expression of ATS features. In the present study, C-terminal mutations were more frequent in the typical ATS group (Table 3). Zhang et al[14] also reported that dysmorphism and periodic paralysis were more frequently observed in C-terminal mutation carriers. The Kir 2.1 C-terminus relates to various types of loss of function in $I_{K1}$ currents. Lopes et al[31] identified 12 basic residues in Kir2.1 that changed channel-$PIP_2$ interactions—10 of them were located in the C-terminus. The C-terminus also contains the endoplasmic reticulum (ER) export sequence, FCYENE, and the trafficking-related acidic cluster EEDDSE at positions 374 to 379 and 386 to 391, respectively.[32,33] More recently, we reported an S369X mutation located close to this ER export signal that impedes ER-Golgi transport.[7]

We tested the trafficking function of four mutations, and only G144D mutation showed a trafficking defect (Figure 5). Our results suggest that the phenotype expression variability of *KCNJ2* mutations may be influenced by the topological location of mutations; however, the other possibilities, for example, environmental factors, modifier genes, or SNPs,[34] remain unstudied.

## Phenotypic Overlap Between CPVT and ATS

The prevalence of *KCNJ2* mutation carriers in the CPVT phenotype was lower than in the other phenotypes (Figure 1 and Table 1). Our 2 CPVT probands with *KCNJ2* mutation (G144D, T305S) had first syncope after the age of 30 years, and their ECGs showed bidirectional VT or PVCs at rest as well. In contrast, the age at first syncope of *RyR2*-related CPVT patients was reportedly younger age (mean age of 8 years),[10] and their syncope occurred mainly during exercise but not while resting. These findings, for example, late onset of symptoms and ventricular arrhythmia at rest, may be clues to distinguish between *KCNJ2*-related and *RyR2*- or *CASQ2*-related CPVT. Functional assays revealed that both G144D and T305S exerted dominant negative suppression effects on outward currents when coexpressed with WT Kir2.1 subunits. Apparently, therefore, baseline functional modulation by these mutations was not related to the phenotypic expression of ATS or CPVT.

Recently, a V227F mutation was identified in a patient with the typical CPVT phenotype but without dysmorphism or periodic paralysis.[35] A biophysical assay showed that heterozygous WT/V227F channels were identical to WT channels in function, but stimulation by cAMP-dependent protein kinase A (PKA) significantly downregulated the heterozygous mutant but not WT Kir2.1 currents. This particular type of loss-of-function may explain why the proband displayed the CPVT phenotype. More recently, Barajas-Martinez et al[36] demonstrated the characteristics of their patient with R260P mutation. She showed typical phenotypes of both ATS and CPVT. The $\beta$-blocker nadolol

was first used but ineffective. Her symptoms subsided after treatment with flecainide. She had dysmorphic features and bidirectional VT both at rest and during exercise testing. Functional analysis revealed that R260P mutation had strong dominant negative suppression effects, like that in our G144D case. Regarding our mutations, their modulation by PKA was not examined because they showed a significant loss-of-function at the baseline (Figure 4).

### Phenotype and Channel Function

Although R82W, R82Q, G144D, and T305S were found in patients with an atypical phenotype of ATS (group B), these mutations showed dominant negative suppression effects on outward currents (Figure 4). Therefore, the results obtained for a heterologous expression system did not necessarily correlate with the clinical ATS severity. In this regard, Eckhardt et al[27] identified 4 *KCNJ2* mutations—R67Q, R82W, T75 mol/L, and T305A—in probands lacking the ATS triad and a family history of ATS. Surprisingly, we also identified R67W, R82W/Q, and T305S in group B. Therefore, residues of R67, R82, and T305 may be associated with atypical ATS phenotypes.

### Study Limitations

Regarding CPVT probands, we screened 34 hot-spot exons of the *RyR2* gene. We could not exclude some variants in the remaining exons of *RyR2*. In conclusion, *KCNJ2* gene screening in patients with atypical ATS (only 1 of the ATS features or CPVT) phenotypes is of clinical importance, because 53% of mutation carriers were found to express atypical phenotypes, despite their severity of arrhythmia.

## Acknowledgments

We are grateful to Dr Hitoshi Horigome, University of Tsukuba; Dr Norito Kokubun, Dokkyo Medical University; Dr Nobuyuki Murakoshi, University of Tsukuba; Dr Ichiro Niimura, Niimura Clinic; Dr Yuji Okuyama, Osaka University Graduate School of Medicine; Dr Takahiro Sato, Kanto Medical Center NTT East Corporation; Dr Yoshiaki Takahashi, Takahashi Pediatric and Cardiac Clinic; Dr Jun Yoshimoto, Shizuoka Children's Hospital; and Dr Masao Yoshinaga, National Hospital Organization Kagoshima Medical Center, for the contribution to this survey. We thank Arisa Ikeda for excellent technical assistance.

## Sources of Funding

This work was supported by research grants from the Ministry of Education, Culture, Science, and Technology of Japan (to Dr Horie); National Natural Science Foundation of China (No. 30930105 to Dr Zhou and No 81170176 to Dr Zang); and health science research grants from the Ministry of Health, Labor, and Welfare of Japan for Clinical Research on Measures for Intractable Diseases (to Dr Horie).

## Disclosures

None.

## References

1. Andersen ED, Krasilnikoff PA, Overvad H. Intermittent muscular weakness, extrasystoles, and multiple developmental anomalies: a new syndrome? *Acta Paediatr Scand.* 1971;60:559–564.
2. Tawil R, Ptacek LJ, Pavlakis SG, DeVivo DC, Penn AS, Ozdemir C, et al. Andersen's syndrome: potassium-sensitive periodic paralysis, ventricular ectopy, and dysmorphic features. *Ann Neurol.* 1994;35:326–330.
3. Zaritsky JJ, Eckman DM, Wellman GC, Nelson MT, Schwarz TL. Targeted disruption of Kir2.1 and Kir2.2 genes reveals the essential role of the inwardly rectifying K(+) current in K(+)-mediated vasodilation. *Circ Res.* 2000;87:160–166.
4. Plaster NM, Tawil R, Tristani-Firouzi M, Canun S, Bendahhou S, Tsunoda A, et al. Mutations in Kir2.1 cause the developmental and episodic electrical phenotypes of Andersen's syndrome. *Cell.* 2001;105:511–519.
5. Ai T, Fujiwara Y, Tsuji K, Otani H, Nakano S, Kubo Y, et al. Novel *KCNJ2* mutation in familial periodic paralysis with ventricular dysrhythmia. *Circulation.* 2002;105:2592–2594.
6. Kobori A, Sarai N, Shimizu W, Nakamura Y, Murakami Y, Makiyama T, et al. Additional gene variants reduce effectiveness of beta-blockers in the LQT1 form of long QT syndrome. *J Cardiovasc Electrophysiol.* 2004;15:190–199.
7. Doi T, Makiyama T, Morimoto T, Haruna Y, Tsuji K, Ohno S, et al. A novel *KCNJ2* nonsense mutation, S369X, impedes trafficking and causes a limited form of Andersen-Tawil syndrome. *Circ Cardiovasc Genet.* 2011;4:253–260.
8. Haruna Y, Kobori A, Makiyama T, Yoshida H, Akao M, Doi T, et al. Genotype-phenotype correlations of *KCNJ2* mutations in Japanese patients with Andersen-Tawil syndrome. *Hum Mutat.* 2007;28:208.
9. Tester DJ, Arya P, Will M, Haglund CM, Farley AL, Makielski JC, et al. Genotypic heterogeneity and phenotypic mimicry among unrelated patients referred for catecholaminergic polymorphic ventricular tachycardia genetic testing. *Heart Rhythm.* 2006;3:800–805.
10. Priori SG, Napolitano C, Memmi M, Colombi B, Drago F, Gasparini M, et al. Clinical and molecular characterization of patients with catecholaminergic polymorphic ventricular tachycardia. *Circulation.* 2002;106:69–74.
11. McManis PG, Lambert EH, Daube JR. The exercise test in periodic paralysis. *Muscle Nerve.* 1986;9:704–710.
12. Tristani-Firouzi M, Jensen JL, Donaldson MR, Sansone V, Meola G, Hahn A, et al. Functional and clinical characterization of *KCNJ2* mutations associated with LQT7 (Andersen syndrome). *J Clin Invest.* 2002;110:381–388.
13. Bazett HC. An analysis of the time relations of electro-cardiograms. *Heart.* 1920;7:353–367.
14. Zhang L, Benson DW, Tristani-Firouzi M, Ptacek LJ, Tawil R, Schwartz PJ, et al. Electrocardiographic features in Andersen-Tawil syndrome patients with *KCNJ2* mutations: characteristic T-U-wave patterns predict the *KCNJ2* genotype. *Circulation.* 2005;111:2720–2726.
15. Yan GX, Antzelevitch C. Cellular basis for the normal T wave and the electrocardiographic manifestations of the long-QT syndrome. *Circulation.* 1998;98:1928–1936.
16. Keating M, Atkinson D, Dunn C, Timothy K, Vincent GM, Leppert M. Linkage of a cardiac arrhythmia, the long QT syndrome, and the Harvey Ras-1 gene. *Science.* 1991;252:704–706.
17. Lepeschkin E. The U wave of the electrocardiogram. *Mod Concepts Cardiovasc Dis.* 1969;38:39–45.
18. Jongbloed R, Marcelis C, Velter C, Doevendans P, Geraedts J, Smeets H. dHPLC analysis of potassium ion channel genes in congenital long QT syndrome. *Hum Mutat.* 2002;20:382–391.
19. George CH, Jundi H, Thomas NL, Fry DL, Lai FA. Ryanodine receptors and ventricular arrhythmias: emerging trends in mutations, mechanisms and therapies. *J Mol Cell Cardiol.* 2007;42:34–50.
20. Medeiros-Domingo A, Bhuiyan ZA, Tester DJ, Hofman N, Bikker H, van Tintelen JP, et al. The *RyR2*-encoded ryanodine receptor/calcium release channel in patients diagnosed previously with either catecholaminergic polymorphic ventricular tachycardia or genotype negative, exercise-induced long QT syndrome: a comprehensive open reading frame mutational analysis. *J Am Coll Cardiol.* 2009;54:2065–2074.
21. Itoh H, Shimizu W, Hayashi K, Yamagata K, Sakaguchi T, Ohno S, et al. Long QT syndrome with compound mutations is associated with a more severe phenotype: a Japanese multicenter study. *Heart Rhythm.* 2010;7:1411–1418.
22. Ohno S, Zankov DP, Yoshida H, Tsuji K, Makiyama T, Itoh H, et al. N- and C-terminal *KCNE1* mutations cause distinct phenotypes of long QT syndrome. *Heart Rhythm.* 2007;4:332–340.
23. Hosaka Y, Hanawa H, Washizuka T, Chinushi M, Yamashita F, Yoshida T, et al. Function, subcellular localization and assembly of a novel mutation of *KCNJ2* in Andersen's syndrome. *J Mol Cell Cardiol.* 2003;35:409–415.
24. Zankov DP, Yoshida H, Tsuji K, Toyoda F, Ding WG, Matsuura H, et al. Adrenergic regulation of the rapid component of delayed rectifier K+

current: implications for arrhythmogenesis in LQT2 patients. *Heart Rhythm*. 2009;6:1038–1046.
25. Yoshida H, Horie M, Otani H, Takano M, Tsuji K, Kubota T, et al. Characterization of a novel missense mutation in the pore of *HERG* in a patient with long QT syndrome. *J Cardiovasc Electrophysiol*. 1999;10: 1262–1270.
26. Donaldson MR, Jensen JL, Tristani-Firouzi M, Tawil R, Bendahhou S, Suarez WA, et al. $PIP_2$ binding residues of Kir2.1 are common targets of mutations causing Andersen syndrome. *Neurology*. 2003;60:1811–1816.
27. Eckhardt LL, Farley AL, Rodriguez E, Ruwaldt K, Hammill D, Tester DJ, et al. KCNJ2 mutations in arrhythmia patients referred for LQT testing: a mutation T305A with novel effect on rectification properties. *Heart Rhythm*. 2007;4:323–329.
28. Fodstad H, Swan H, Auberson M, Gautschi I, Loffing J, Schild L, et al. Loss-of-function mutations of the K(+) channel gene *KCNJ2* constitute a rare cause of long QT syndrome. *J Mol Cell Cardiol*. 2004;37:593–602.
29. Liu XK, Katchman A, Drici MD, Ebert SN, Ducic I, Morad M, et al. Gender difference in the cycle length-dependent QT and potassium currents in rabbits. *J Pharmacol Exp Ther*. 1998;285:672–679.
30. Andelfinger G, Tapper AR, Welch RC, Vanoye CG, George AL Jr, Benson DW. KCNJ2 mutation results in Andersen syndrome with sex-specific cardiac and skeletal muscle phenotypes. *Am J Hum Genet*. 2002;71:663–668.
31. Lopes CM, Zhang H, Rohacs T, Jin T, Yang J, Logothetis DE. Alterations in conserved Kir channel-$PIP_2$ interactions underlie channelopathies. *Neuron*. 2002;34:933–944.
32. Nehring RB, Wischmeyer E, Doring F, Veh RW, Sheng M, Karschin A. Neuronal inwardly rectifying K(+) channels differentially couple to PDZ proteins of the PSD-95/SAP90 family. *J Neurosci*. 2000;20:156–162.
33. Ma D, Zerangue N, Raab-Graham K, Fried SR, Jan YN, Jan LY. Diverse trafficking patterns due to multiple traffic motifs in g protein-activated inwardly rectifying potassium channels from brain and heart. *Neuron*. 2002;33:715–729.
34. Pfeufer A, Jalilzadeh S, Perz S, Mueller JC, Hinterseer M, Illig T, et al. Common variants in myocardial ion channel genes modify the qt interval in the general population: results from the KORA study. *Circ Res*. 2005;96:693–701.
35. Vega AL, Tester DJ, Ackerman MJ, Makielski JC. Protein kinase A-dependent biophysical phenotype for V227F-*KCNJ2* mutation in catecholaminergic polymorphic ventricular tachycardia. *Circ Arrhythm Electrophysiol*. 2009;2:540–547.
36. Barajas-Martinez H, Hu D, Ontiveros G, Caceres G, Desai M, Burashnikov E, et al. Biophysical and molecular characterization of a novel de novo *KCNJ2* mutation associated with Andersen-Tawil syndrome and catecholaminergic polymorphic ventricular tachycardia mimicry. *Circ Cardiovasc Genet*. 2011;4:51–57.

## CLINICAL PERSPECTIVE

Mutations of *KCNJ2*, the gene encoding the human inward rectifier potassium channel Kir2.1, cause Andersen-Tawil syndrome (ATS), a disease exhibiting ventricular arrhythmia, periodic paralysis and dysmorphic features. However, some *KCNJ2* mutation carriers lack the ATS triad and sometimes share the phenotype of catecholaminergic polymorphic ventricular tachycardia (CPVT). We focused on the *KCNJ2* mutation carriers with "atypical ATS phenotype"—patients showing only 1 of ATS features and CPVT phenotype. We investigated the prevalence, clinical, and biophysical characteristics of "atypical ATS" phenotype in *KCNJ2* mutation carriers. *KCNJ2* screening were performed in 57 unrelated probands showing typical (≥2 ATS features) and atypical ATS. We identified 24 *KCNJ2* mutation carriers. Mutation-positive rates were 75% (15/20) in typical ATS, 71% (5/7) in ATS cardiac phenotype alone, 100% (2/2) in periodic paralysis alone, and 7% (2/28) in CPVT. Including 24 *KCNJ2* mutation-positive family members, we divided all carriers (n=45) into 2 groups: typical ATS (A) (n=21, 47%) and atypical phenotype (B) (n=24, 53%). Patients in (A) had a longer QUc interval and higher U-wave amplitude. C-terminal mutations were more frequent in (A). There were no significant differences in incidences of ventricular tachycardia. In patch-clamp analysis using heterologous expression system, the outward IK1 currents of 4 mutations found in (B) showed dominant negative suppression effect although their mild ATS phenotype. *KCNJ2* gene screening in atypical ATS phenotypes is of clinical importance, because more than half (53%) of mutation carriers express atypical phenotypes, despite their arrhythmia severity.

Cardiovascular Research (2012) **95**, 419–429
doi:10.1093/cvr/cvs206

# Disease characterization using LQTS-specific induced pluripotent stem cells

**Toru Egashira[1], Shinsuke Yuasa[1,2]*, Tomoyuki Suzuki[1,3], Yoshiyasu Aizawa[1], Hiroyuki Yamakawa[1], Tomohiro Matsuhashi[1], Yohei Ohno[1], Shugo Tohyama[1], Shinichiro Okata[4], Tomohisa Seki[1], Yusuke Kuroda[1,3], Kojiro Yae[1], Hisayuki Hashimoto[1], Tomofumi Tanaka[1,5], Fumiyuki Hattori[1,5], Toshiaki Sato[1], Shunichiro Miyoshi[1], Seiji Takatsuki[1], Mitsushige Murata[1,6], Junko Kurokawa[4], Tetsushi Furukawa[4], Naomasa Makita[7], Takeshi Aiba[8], Wataru Shimizu[8], Minoru Horie[9], Kaichiro Kamiya[3], Itsuo Kodama[3], Satoshi Ogawa[1], and Keiichi Fukuda[1]***

[1]Department of Cardiology, Keio University School of Medicine, 35 Shinanomachi, Shinjuku, Tokyo 160-8582, Japan; [2]Center for Integrated Medical Research, Keio University School of Medicine, 35 Shinanomachi, Shinjuku, Tokyo 160-8582, Japan; [3]Department of Cardiovascular Research, Research Institute of Environmental Medicine, Nagoya University, Nagoya, Japan; [4]Department of Bio-informational Pharmacology, Medical Research Institute, Tokyo Medical and Dental University, Tokyo, Japan; [5]Asubio Pharma Co., Ltd, Hyogo, Japan; [6]Department of Laboratory Medicine, Keio University School of Medicine, Tokyo, Japan; [7]Department of Molecular Physiology-1, Nagasaki University Graduate School of Biomedical Sciences, Nagasaki, Japan; [8]Division of Arrhythmia and Electrophysiology, Department of Cardiovascular Medicine, National Cerebral and Cardiovascular Center, Osaka, Japan; and [9]Department of Cardiovascular Medicine, Shiga University of Medical Science, Shiga, Japan

*Received 30 November 2011; revised 9 June 2012; accepted 19 June 2012; online publish-ahead-of-print 27 June 2012*

**Time for primary review: 26 days**

**Aims** Long QT syndrome (LQTS) is an inheritable and life-threatening disease; however, it is often difficult to determine disease characteristics in sporadic cases with novel mutations, and more precise analysis is necessary for the successful development of evidence-based clinical therapies. This study thus sought to better characterize ion channel cardiac disorders using induced pluripotent stem cells (iPSCs).

**Methods and results** We reprogrammed somatic cells from a patient with sporadic LQTS and from controls, and differentiated them into cardiomyocytes through embryoid body (EB) formation. Electrophysiological analysis of the LQTS-iPSC-derived EBs using a multi-electrode array (MEA) system revealed a markedly prolonged field potential duration (FPD). The IKr blocker E4031 significantly prolonged FPD in control- and LQTS-iPSC-derived EBs and induced frequent severe arrhythmia only in LQTS-iPSC-derived EBs. The IKs blocker chromanol 293B did not prolong FPD in the LQTS-iPSC-derived EBs, but significantly prolonged FPD in the control EBs, suggesting the involvement of IKs disturbance in the patient. Patch-clamp analysis and immunostaining confirmed a dominant-negative role for 1893delC in IKs channels due to a trafficking deficiency in iPSC-derived cardiomyocytes and human embryonic kidney (HEK) cells.

**Conclusions** This study demonstrated that iPSCs could be useful to characterize LQTS disease as well as drug responses in the LQTS patient with a novel mutation. Such analyses may in turn lead to future progress in personalized medicine.

**Keywords** Long QT syndrome • Drug examination • iPS cells • Cardiomyocytes • Personalized medicine

## 1. Introduction

Sudden cardiac arrest (SCA) is a major cause of mortality in developed countries, accounting for about 10% of all deaths.[1] The majority of sudden cardiac deaths are caused by acute ventricular tachyarrhythmias,[2] which often occur in persons without known cardiac disease, structural heart disease, or coronary artery disease.[3–6] Long QT syndrome (LQTS) was initially described as a rare inherited disease causing ventricular tachyarrhythmia. Subsequently, many patients have been identified and now we know that ventricular tachyarrhythmia in LQTS is apparently common among sudden death syndromes. The reported incidence of LQTS is one in 2000, but this may underestimate the disease because many cases are not properly diagnosed because of the rarity of the condition and the wide spectrum of symptoms.[7]

* Corresponding author. Tel: +81 3 5363 3874 (K.F.)/+81 3 5363 3373 (S.Y.); fax: +81 3 5363 3875 (K.F.), Email: kfukuda@sc.itc.keio.ac.jp (K.F.)/ yuasa@a8.keio.jp (S.Y.).

Human-induced pluripotent stem cells (hiPSCs) have become a promising tool for analysing human genetic diseases.[8,9] Many studies have already shown that apparent cellular phenotypes of familial genetic disorders are recapitulated by disease-specific iPSC-derived cells *in vitro*. In some of these, cardiomyocytes differentiated from LQTS-specific iPSCs (LQTS-iPSCs) were used to recapitulate disease phenotypes in LQTS patients who were previously characterized as having mutated channel profiles.[10–13] In reality, many patients have novel mutations and no such specific information regarding their disease phenotype is matched by the respective genotypes. To address whether iPSC technology could be used to characterize a novel mutated gene, we selected LQTS patients without family history and previous disease characterization.

# 2. Methods

## 2.1 Human iPSC generation

iPSCs were established as described previously.[8] We used lentiviral to introduce mouse solute carrier family 7, a member 1 (*Slc7a1*) gene encoding the ecotropic retrovirus receptor. Transfectants were plated at $2 \times 10^5$ cells per 60 mm dish. The next day, *OCT3/4*, *SOX2*, *KLF4*, and *c-MYC* were introduced by retroviral. Twenty four hours after transduction, aspirated off the virus-containing medium, then continued to culture under fibroblast condition. Six days later, the cells were harvested and plated at $5 \times 10^4$ cells per 100 mm dish. The cells were cultured for another 20 days. At day 25, embryonic stem cell-like colonies were mechanically dissociated and transferred to a 24-well plate on the mouse embryonic fibroblast feeders.

## 2.2 Patient consent

All subjects provided informed consent for blood testing for genetic abnormalities associated with hereditary LQTS. Isolation and use of patient and control fibroblasts was approved by the Ethics Committee of Keio University (20-92-5), and performed only after written consent was obtained. Our study also conforms with the principles outlined in the Declaration of Helsinki for use of human tissue or subjects.[14]

## 2.3 *In vitro* differentiation

Cells were harvested using 1 mg/ml collagenase IV (Invitrogen, CA, USA), and transferred to ultra-low attachment plates (Corning, NY, USA) in differentiation medium.[15] The medium was replaced every second day. The time window of differentiation for analysing the beating embryoid bodies (EBs) and cardiomyocytes was 30–60 days and 150 days from starting the differentiating conditions.

## 2.4 Immunofluorescence

The immunostaining was performed using the following primary antibodies and reagents: anti-OCT3/4 (sc-5279, Santa Cruz, CA, USA), anti-E-cadherin (M108, TAKARA BIO, Otsu, Japan), anti-NANOG (RCAB0003P, ReproCELL, Yokohama, Japan), anti-SSEA 1(sc-21702, Santa Cruz), anti-SSEA 3 (MAB4303, Millipore, MA, USA), anti-SSEA 4 (MAB4304, Millipore), anti-Tra1-60 (MAB4360, Millipore), anti-Tra1-81 (MAB4381, Millipore), anti-α-Actinin (A7811, Sigma-Aldrich, MO, USA), anti-ANP (sc-20158, Santa Cruz), anti-MHC (MF20, Developmental Studies Hybridoma Bank, IA, USA), anti-TNNT (13-11, Thermo Scientific, NeoMarkers, MA, USA), anti-GATA4 (sc-1237, Santa Cruz), anti-NKX2.5 (sc-8697, Santa Cruz), anti-KCNQ1 (s37A-10, ab84819, Abcam, Cambridgeshire, UK), anti-WT-KCNQ1 (APC-022, Alomone Labs, Jerusalem, Israel), fluorescent phallotoxins (A22283, Molecular Probes, OR, USA), Wheat Germ Agglutinin Conjugates[16,17] (W11262, Molecular Probes) and DAPI (Molecular Probes). Signal was detected using a conventional fluorescence laser microscope (BZ-9000, KEYENCE, Osaka, Japan) equipped with a colour charge-coupled device camera (BZ-9000, KEYENCE).

## 2.5 Reverse transcription–polymerase chain reaction

Total RNA samples were isolated using the TRIZOL reagent (Invitrogen) and RNase-free DNase I (Qiagen, Tokyo, Japan). cDNAs were synthesized using the Superscript First-Strand Synthesis System (Invitrogen). Real-time quantitative reverse transcription–polymerase chain reaction (RT–PCR) was performed using 7500 Real-Time PCR System (Applied Biosystems, CA, USA), with SYBR Premix ExTaq (Takara, Otsu, Japan). The amount of mRNA was normalized to GAPDH mRNA. Primer sequences are listed in the Supplementary material online, *Table*.

## 2.6 Teratoma formation

The mice were anaesthetized using a mixture of ketamine (50 mg/kg), xylazine (10 mg/kg), and chlorpromazine (1.25 mg/kg). The adequacy of anaesthesia was monitored by heart rate, muscle relaxation, and the loss of sensory reflex response, i.e. non-response to tail pinching. hiPSCs (at a concentration corresponding to 25% of the cells from a confluent 150 mm dish) were injected into the testis of severe combined immunodeficiency disease (SCID) mice (CREA Japan, Tokyo, Japan). At 6–8 weeks post-injection, teratomas were dissected, fixed in 10% paraformaldehyde overnight, and embedded in paraffin. The sections were stained with haematoxylin and eosin. All experiments were performed in accordance with the Keio University animal care guidelines and approved by the Ethics Committee of Keio University (20-041-4), which conforms to the Guide for the Care and Use of Laboratory Animals published by the US National Institutes of Health (NIH Publication no. 85-23, revised 1996).

## 2.7 Karyotype analysis

Karyotype analysis was performed using standard Q-banding chromosome analysis according to the Central Institute for Experimental Animals.

## 2.8 Genomic sequence

Genomic DNA was isolated from the patient, control volunteers, control iPSC colonies, and LQTS-iPSC colonies. The relevant *KNCQ1* gene fragment was amplified by PCR reaction using 100 ng genomic DNA. PCR products were then sequenced.

## 2.9 Cell culture and transient transfection

Human embryonic kidney (HEK) cells were obtained from the American Type Cell Collection and seeded in 35 mm dishes 1 day before transfection and then transfected with various plasmids using FuGENE 6 Transfection Reagent (Roche Applied Science, Penzberg, Germany). Aliquots of 1 or 0.5 μg of WT-*KCNQ1* and/or 1 or 0.5 μg of P631fs/33-*KCNQ1*, together with 1 μg of WT-*KCNE1* and 0.2 μg of GFP, were transfected into HEK cells. Cells were studied at 48–72 h after transfection.

## 2.10 Field potential recordings using the on-chip multi-electrode array system

Multi-electrode array (MEA) chips from Multi Channel Systems (Germany) were coated with fibronectin (F1141; Sigma-Aldrich). EBs were plated and incubated at 37°C. MEA measurements were performed at 37°C. The signals were initially processed, and the obtained data were subsequently analysed with MC_Rack (Multi Channel Systems). Data for analysis were extracted from 2–5 min of the obtained data. The recorded extracellular electrograms were used to determine local field potential duration (FPD), defined as the time interval between the initial deflection of the FP and the maximum local T wave. FPD measurements were normalized (corrected FPD: cFPD) to the activation rate using Bazett's correction formulae: $cFPD = FPD/(RR\ interval)^{1/2}$, where RR indicates the time interval (in seconds) between two consecutive beats.[18] E4031

(M5060; Sigma-Aldrich), chromanol 293B (C2615; Sigma-Aldrich), barium chloride (Fluka 34252; Sigma-Aldrich), isoproterenol hydrochloride (I6504; Sigma-Aldrich), and propranolol hydrochloride (P0884; Sigma-Aldrich) were prepared as 1 or 10 mM stock solutions. The FPs were recorded for 5 min. Drug was then added to the medium. After 5–10 min of incubation, the FPs were measured for 5–10 min. MEA recordings were performed by investigators blinded to the genotype of the cells.

### 2.11 Whole-cell patch-clamp electrophysiology

The external solution used to measure $K^+$ currents in iPSC-derived cardiomyocytes was composed of the following (in mM): *N*-methyl-D-glucamine 149, $MgCl_2$ 5, HEPES 5, and nisoldipine 0.003. IKs were separated by applying chromanol 293B. In HEK cells, Tyrode's solution used to measure KCNQ1 channel currents comprised (in mM): NaCl 143, KCl 5.4, $CaCl_2$ 1.8, $MgCl_2$ 0.5, $NaH_2PO_4$ 0.25, HEPES 5.0, and glucose 5.6; pH was adjusted to 7.4 with NaOH. The glass pipette had a resistance of 3–5 MΩ after filling with the internal pipette solution containing (in mM) KOH 60, KCl 80, aspartate 40, HEPES 5, EGTA 10, Mg ATP 5, sodium creatinine phosphate 5, and $CaCl_2$ 0.65; pH 7.2. KCNQ1 channel currents were recorded using Axopatch 200B, Digidata 1440A, and pClamp 10.2 (Axon Instruments, Foster City, CA, USA) for data amplification, acquisition, and analysis, respectively. For $K^+$ current measurement in iPSC-derived cardiomyocytes, depolarizing pulses for 3 s from −60 to 60 mV were applied from the holding potential at −60 mV at 0.1 Hz. The tail current was measured on repolarization back to −40 mV. KCNQ1 channel currents were elicited by 3 s depolarizing steps from a holding potential of −80 mV to potentials ranging from −50 to +60 mV in 10 mV increments. This was followed by a 2 s repolarization phase to −40 mV to elicit the tail current. Pulse frequency was 0.1 Hz. Whole-cell patch-clamp recordings were performed by investigators blinded to the genotype of the cells.

### 2.12 Statistical analysis

Data are expressed as mean ± SEM. Unless otherwise noted, statistical significance was assessed with Student's *t*-test and Fischer's exact test for simple comparisons, and ANOVA followed by Bonferroni's test for multiple comparisons. The probability level accepted for significance was $P < 0.05$ ($^*P < 0.05$, $^{**}P < 0.01$).

## 3. Results

A 13-year-old boy was admitted to our institution with SCA experienced during physical exercise at school. He subsequently underwent successful resuscitation using an automated external defibrillator , the data from which showed ventricular fibrillation, a fatal arrhythmic event (see Supplementary material online, *Figure S1A*). Electrocardiogram showed a significantly prolonged QT interval and QT interval corrected for heart rate, QTc (see Supplementary material online, *Figure S1B*). He had no family history of previous syncope episodes or significant QT interval abnormality (see Supplementary material online, *Figure S1C*). Since the clinical findings on syncope and the electrocardiogram morphology suggested type 1 LQTS, β-blockers were initially administered to reduce the risk of cardiac sudden death.[19] The epinephrine provocation test increases the accuracy of diagnosis of type 1 LQTS;[20] however, this test can be affected by β-blocker administration (see Supplementary material online, *Figure S1D*); thus, type 1 LQTS being the most probable diagnosis in our patient was not definitive.[21] To elucidate whether this patient is type 1 LQTS caused by a *KCNQ1* mutation, *KCNQ1* was directly sequenced. A heterozygous deletion mutant in *KCNQ1*, 1893delC (P631fs/33), was identified in our patient (see Supplementary material online, *Figure S1E* and *F*). We also confirmed that no other mutation was present in the major LQTS-related genes: *KCNH2*, *SCN5A*, *KCNE1*, and *KCNE2*. Although the *KCNQ1* 1893delC mutation was previously reported, its functional characteristics remain unknown.[22] To obtain electrophysiological properties, drug responses, and some valid data on which to base useful medical therapy, we tested the validity of iPSCs for disease characterization.

To generate iPSCs, we used dermal fibroblasts from our patient and two healthy volunteers, and reprogrammed these cells using retrovirus-mediated gene transfer of *SOX2*, *OCT3/4* (also known as *POU5F1*), *KLF4*, and *MYC*. Several clones were generated, expanded, and stored. All iPSC lines showed typical iPSC morphology and expressed human pluripotency markers (*Figure 1A* and *B*). Quantitative RT–PCR (qRT–PCR) analyses confirmed that all lines adequately expressed endogenous pluripotency markers and silenced exogenous genes (*Figure 1C* and *D*). To examine pluripotency, iPSCs were injected into SCID mice. Injected iPSC-derived teratomas contained the cell derivatives of all three germ layers, such as cartilage, intestine, muscle, and neural tissue (see Supplementary material online, *Figure S2A* and *B*). All iPSC lines maintained a normal karyotype (see Supplementary material online, *Figure S2C* and *D*). We selected two LQTS and two control iPSC lines for further characterization and cardiac differentiation.

We used an EB culture system to differentiate iPSCs into cardiomyocytes.[15,23] After 1 week of floating culture, spontaneous beating EBs were observed, and the efficiency of beating EBs showed no significant difference between control- and LQTS-iPSCs at days 30 and 60 (data not shown). Immunofluorescence staining for dissociated cardiomyocytes showed clear immunopositivity for cardiac-specific gene products in control- and LQTS-iPSC-derived cardiomyocytes (*Figure 2A* and *B*). Electron microscopy also revealed a typical cardiomyocyte structure in both control- and LQTS-iPSC-derived cardiomyocytes, including sarcomeric organization and gap junctions (see Supplementary material online, *Figure S3A* and *B*). Similarly, qRT–PCR analyses confirmed the expression of cardiac-specific genes and ion channels (*Figure 2C*). Ion channel expression in iPSCs was compatible with previous reports of multiple ion channels expressed in pluripotent stem cells.[24,25] To elucidate electrophysiological properties, we used an MEA system that enables easy measurement of the surface electrogenic activities of cell clusters and can be adapted to automatic high-throughput systems.[26] MEA analyses revealed that control- and LQTS-iPSC-derived EBs showed similar rhythmic electrical activity and spontaneous beating rate (*Figure 3A* and *B*). FPD in MEA analysis is analogous to a QT interval in an electrocardiogram.[26] The cFPD (normalized to beating frequency) of LQTS-iPSC-derived EBs was significantly longer than that of controls (*Figure 3C* and *D*), suggesting that iPSC-derived cardiomyocytes from both control and LQTS cells have cardiac-specific functional properties.

We next tested several drugs known to affect QT prolongation to elucidate the electrophysiological properties of EBs. The IKr blocker, E4031, significantly prolonged cFPD in a dose-dependent manner when added into the culture medium of control and LQTS cells (*Figure 4A* and *B*). E4031 administration induced significantly more frequent early-after depolarizations (EADs) in the LQTS-iPSC-derived beating EBs compared with the control EBs; these are spontaneous membrane depolarizations that confer risk of ventricular arrhythmias (*Figure 4C* and Supplementary material online, *Figure S4A*). In addition, higher doses of E4031 induced arrhythmic events such as

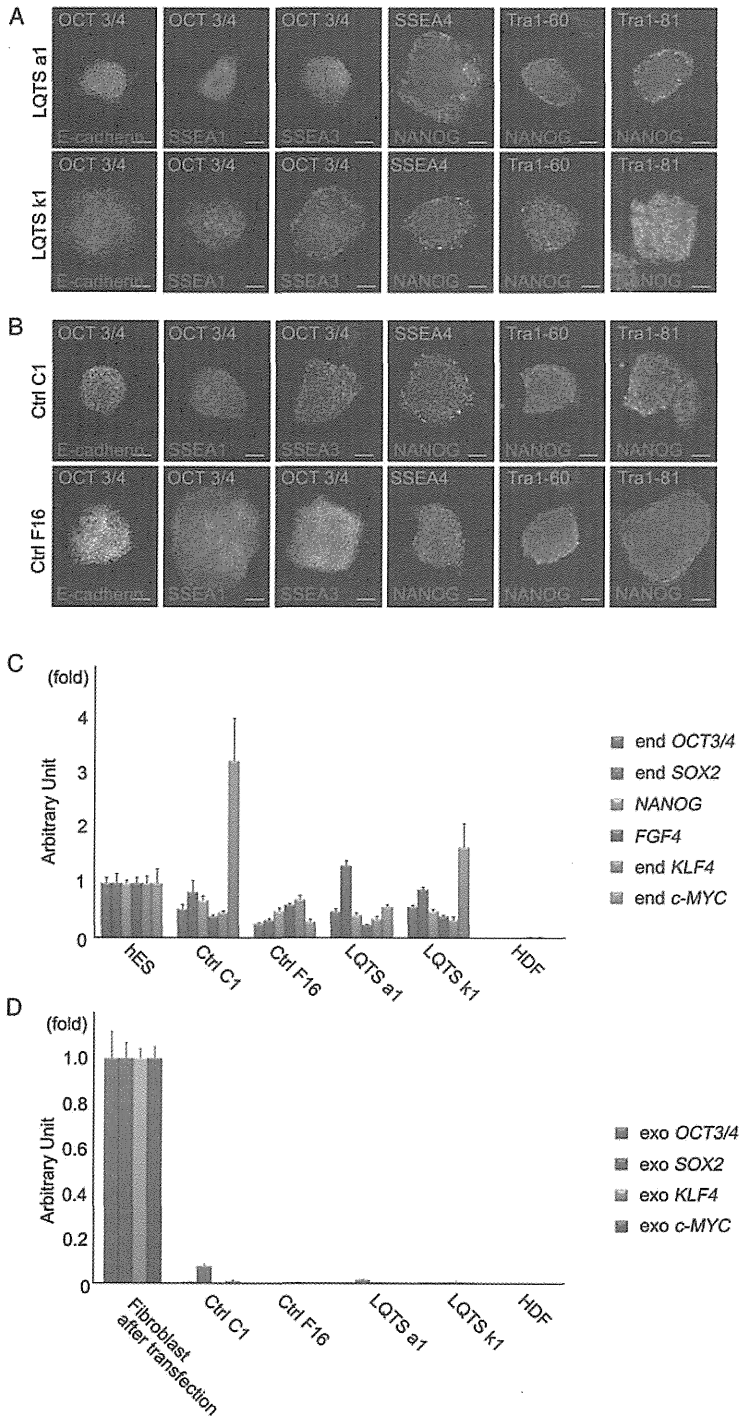


**Figure 1** Generation of iPSCs from a patient with LQTS. (*A*) Immunofluorescence staining for stem cell markers (OCT3/4, E-cadherin, NANOG, SSEA3, SSEA4, Tra1-60 and Tra1-81) in LQTS-iPSC colonies. SSEA1 is not a stem cell marker in hiPSCs. Scale bar, 100 μm. (*B*) Immunofluorescence staining for stem cell markers in control-iPSC colonies. Scale bar, 100 μm. (*C*) Quantitative RT–PCR analyses for endogenous *OCT3/4*, endogenous *Sox2*, endogenous *KLF4*, endogenous *c-MYC*, and *NANOG* and *FGF4* in hES, control-iPSC, LQTS-iPSC, and human dermal fibroblasts (HDF). (*D*) Quantitative RT–PCR analyses for exogenous *OCT3/4*, exogenous *Sox2*, exogenous *KLF4* and exogenous *c-MYC* in HDF at 6 days after transfection, control-iPSC, LQTS-iPSC, and HDF.

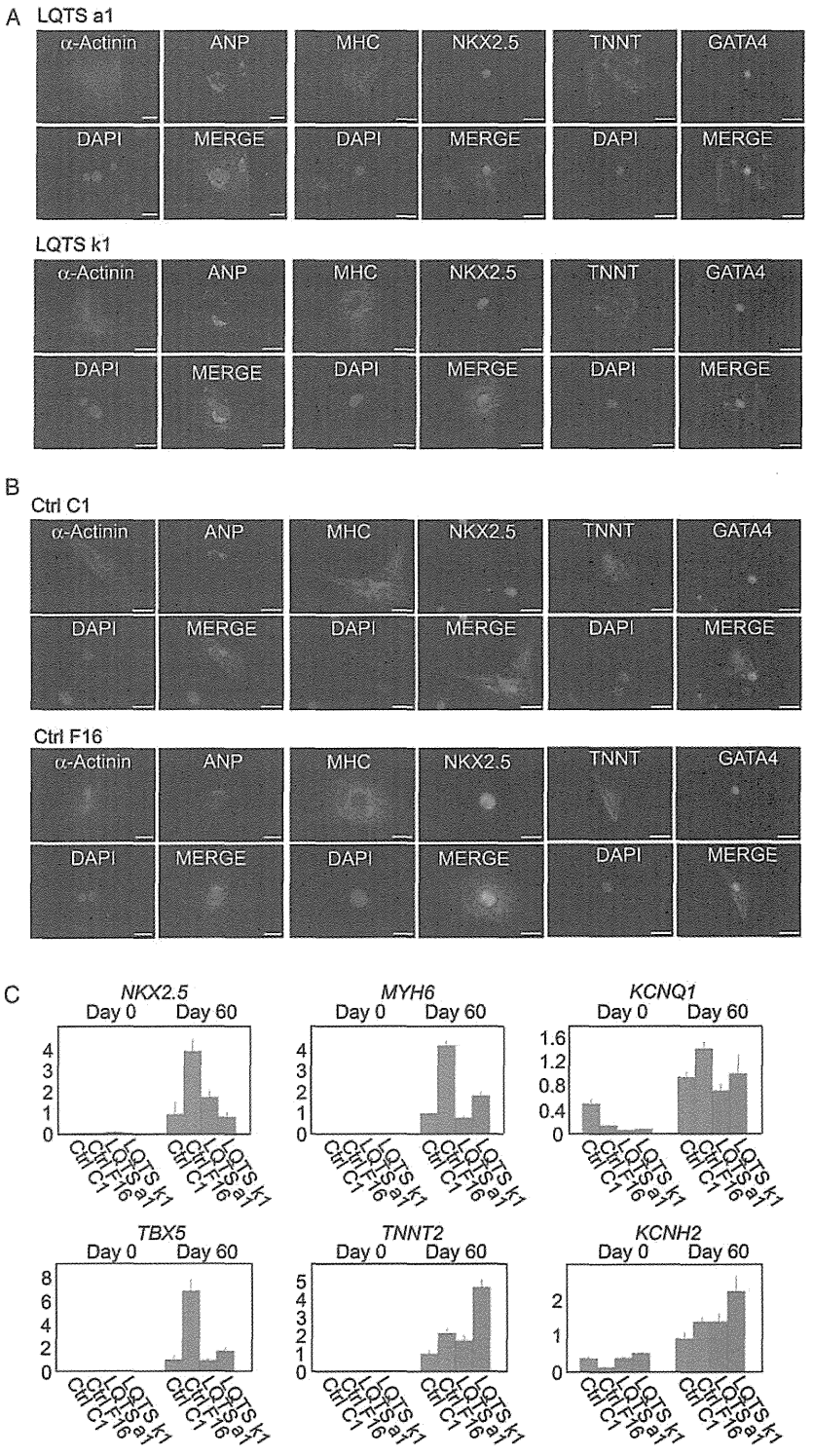


**Figure 2** Cardiomyocyte generation from control- and LQTS-iPSCs. (*A*) and (*B*) Immunofluorescence staining for cardiac markers (α-Actinin, ANP, MHC, NKX2.5, GATA4, and TNNT) in the LQTS- and control-iPSC-derived cardiomyocytes. Scale bar, 20 μm. (*C*) Quantitative RT–PCR analyses for cardiac markers (*NKX2.5*, *TBX5*, *MYH6*, and *TNNT2*) and ion channels (*KCNQ1* and *KCNH2*) in the control- (Ctrl) and LQTS-iPSC, and in iPS-derived EBs at day 60.

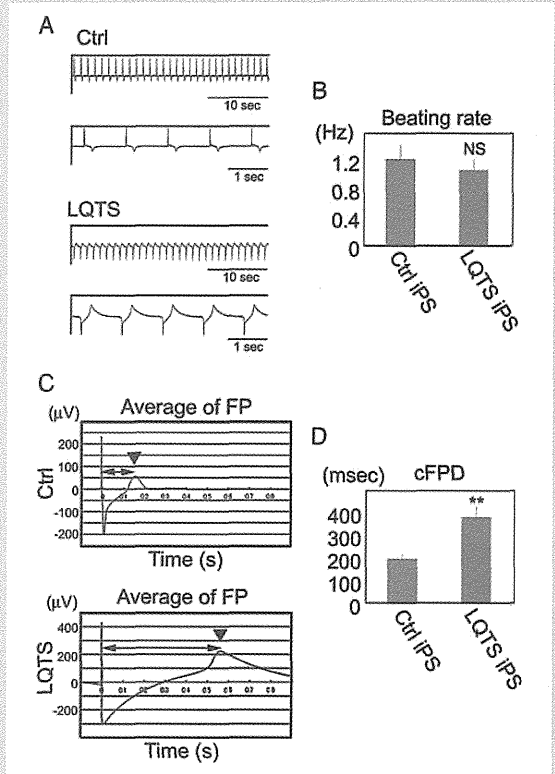


**Figure 3** Electrophysiological features of LQTS-iPSC-derived cardiomyocytes. (*A*) Representative MEA recording from the control- and LQTS-iPSC-derived beating EBs. (*B*) Beating rate of the control- and LQTS-iPSC-derived EBs. (*C*) Average of field potential (FP) recorded by MEA in the control- ($n = 12$) and LQTS-iPSC-derived beating EBs ($n = 12$). Triangle indicates the peak of FP and bilateral arrow indicates the FPD. (*D*) cFPD obtained from the control- ($n = 12$) and LQTS-iPSC-derived beating EBs ($n = 12$).

polymorphic ventricular tachycardia (PVT)-like arrhythmia (*Figure 4D* and Supplementary material online, *Figure S4A*).[27] E4031-induced PVT-like arrhythmias were never observed in control-iPSC-derived beating EBs. We then found that another major repolarization potassium current relating to LQTS, IKs, was blocked by chromanol 293B, which significantly prolonged cFPD in control-iPSC-derived beating EBs, but not in LQTS-iPSC-derived beating EBs (*Figure 4E* and *F*). These data indicated that LQTS-iPSC-derived cardiomyocytes have IKs channel dysfunction and/or chromanol 293B insensitivity. We also examined the inwardly rectifying potassium current IK1 by the IK1-blocking barium administration. The application of barium prolonged FPD in both control- and LQTS-iPSC-derived cardiomyocytes (see Supplementary material online, *Figure S4B*). However, barium administration did not induce arrhythmogenic events in control- and LQTS-iPSC-derived beating EBs. These findings suggested that repolarization of LQTS-iPSC-derived cardiomyocytes would be mainly controlled by IKr. Taken together with IKr and IKs blocker administration, we proposed that IKs channels were not only genetically but functionally impaired and that IKr channels compensated for this effect in the patient-derived iPSCs, which is also known as the repolarization reserve in cardiomyocytes.[28,29] IKs channel impairment is diagnosed as type 1 LQTS. And it is well known that β-stimulant increases the risk of fatal arrhythmia and that β-blockers would effectively prevent long-QT-related arrhythmia in type1 LQTS.[30] The β-stimulant isoproterenol increased the beating rate in a dose-dependent manner in control and LQTS cells, and induced EAD and ventricular tachycardia (VT)-like arrhythmogenic events in LQTS-iPSC-derived beating EBs (see Supplementary material online, *Figure S5A* and *B* and *Figure 4G*). Interestingly, the non-selective β-blocker propranolol obviously decreased the incidence of arrhythmogenic events (*Figure 4H*). These data strongly suggested that our patient has a functional impairment in the IKs channel system. We confirmed a heterozygous deletion mutant in KCNQ1, 1893delC (P631fs/33), was identified in the LQTS-iPSCs (see Supplementary material online, *Figure S5C*).

To confirm a possible dominant-negative role of the *KCNQ1* 1893delC mutation in IKs channel function, we conducted precise electrophysiological characterizations in iPSC-derived cardiomyocytes. IKs currents can be recorded by subtraction of baseline and the IKs blocker (chromanol 293B) addition. In control, chromanol 293B (30 μM) addition apparently decreased the recorded current, and IKs current was recorded by subtraction (*Figure 5A*). In LQTS-derived cardiomyocytes, chromanol 293B addition did not show apparent differences and IKs current was subtly recorded by subtraction (*Figure 5A*). The IKs peak and tail current densities of the LQTS-derived cardiomyocytes were evidently smaller than those of control (*Figure 5B*). To clarify the mechanisms underlying such effects, we examined KCNQ1 protein expression in LQTS-iPSC-derived cardiomyocytes. We conducted immunofluorescent staining using an antibody that recognizes a C-terminal epitope on *KCNQ1* downstream of P631fs/33. Immunostaining in control showed cell peripheral expression of KCNQ1, which suggested normal shuttling of the KCNQ1 protein into the cell membrane (*Figure 5C*). In LQTS-iPSC-derived cardiomyocytes, the KCNQ1 protein was accumulated at the perinuclear cytoplasm and nucleus, instead of at the cell periphery (*Figure 5C*). These data indicated that KCNQ1 expression is downregulated at the membrane peripheral site (*Figure 5D*), which suggests that KCNQ1 1893delC has a dominant-negative effect via a trafficking deficiency.

We showed this patient has a mutation in *KCNQ1* and that LQTS-iPSC-derived cardiomyocytes have a functional disturbance in KCNQ1 channels. However, it remains unclear whether this mutation directly contributed and whether other mutations could be involved in the IKs current disturbance. To test for a pure dominant-negative role of the *KCNQ1* 1893delC mutation in IKs channel function, we also conducted electrophysiological and histochemical characterizations in HEK cells expressing exogenous wild-type and/or mutated KCNQ1. Cells with 100% incorporation of the wild-type *KCNQ1* (WT) gene recorded typical IKs currents and 50% WT *KCNQ1* gene introduction slightly reduced the IKs currents (*Figure 6A*). Introduction of 100% mutant *KNCQ1* genes (P631fs/33) (MT) significantly reduced IKs currents (*Figure 6A*). Moreover, 50% WT and 50% MT gene introductions had dominant-negative effects on IKs current (*Figure 6A*). The IKs peak and tail current densities of the 100% MT and 50/50% WT and MT were evidently smaller than those of 100% WT and 50% WT (*Figure 6B* and *C*). Then we also examined KCNQ1 protein expression in *KCNQ1*-transfected HEK cells. Cells

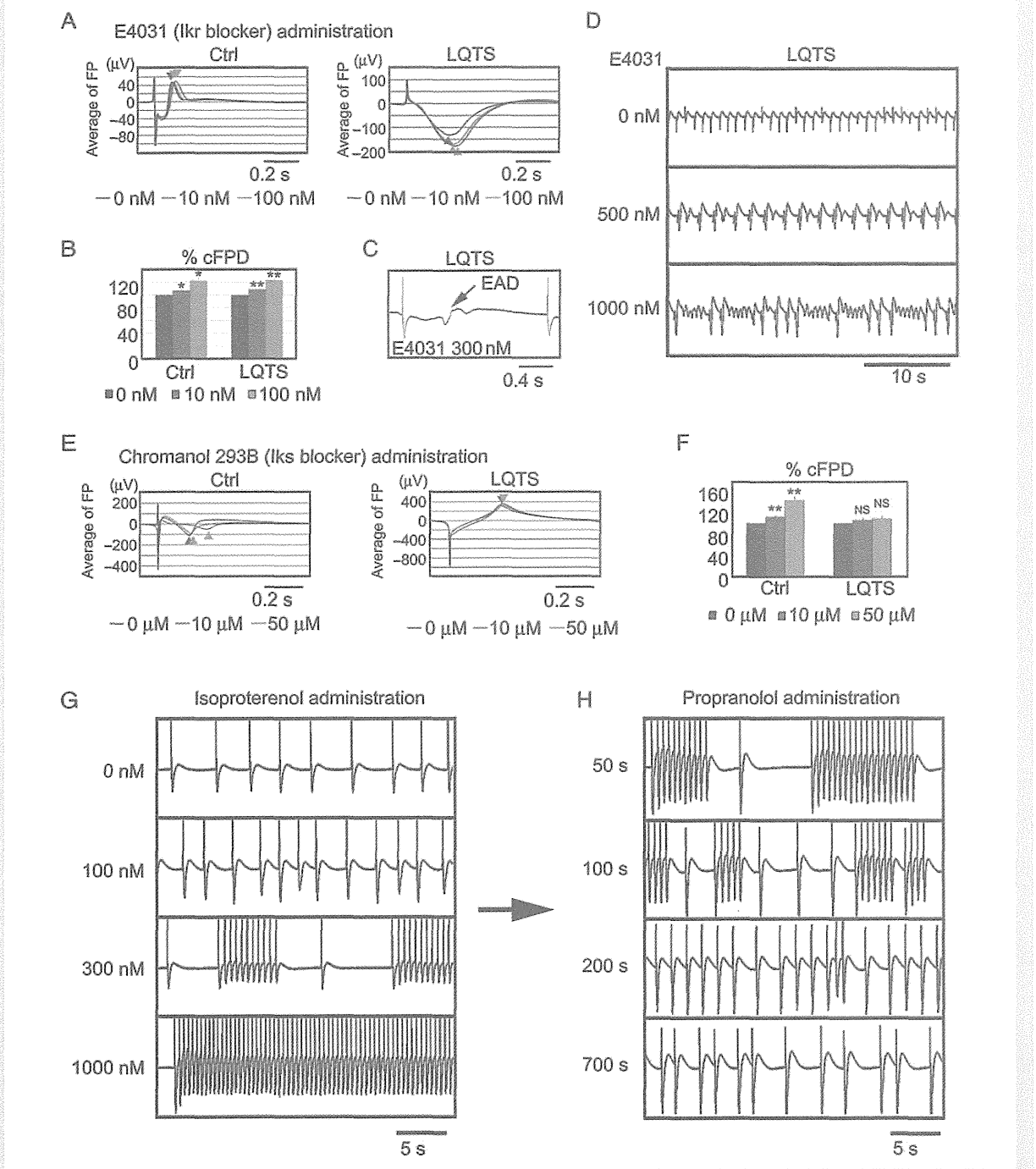


**Figure 4** Drug responses of LQTS-iPSC-derived cardiomyocytes. (*A*) Average of FP recorded by MEA after E4031 administration in the control- and LQTS-iPSC-derived beating EBs. Triangle indicates the peak of FP. (*B*) Per cent change of cFPD after E4031 administration obtained from the control- ($n = 6$) and LQTS-iPSC-derived beating EBs ($n = 6$). (*C*) Representative MEA recordings showing EAD after E4031 administration in LQTS-iPSC-derived beating EBs. The frequency of appearing EAD in each cell is control- ($n = 1/16$) and LQTS-iPSC-derived beating EBs ($n = 8/16$). (*D*) Representative MEA records showing PVT-like arrhythmia after E4031 administration in LQTS-iPSC-derived beating EBs. (*E*) Average of FP recorded by MEA after chromanol 293B administration in the control- and LQTS-iPSC-derived beating EBs. Triangle indicates the peak of FP. (*F*) Per cent change of cFPD after chromanol 293B administration obtained from the control- ($n = 8$) and LQTS-iPSC-derived beating EBs ($n = 8$). (*G*) Representative MEA records showing VT-like arrhythmia after isoproterenol administration in LQTS-iPSC-derived beating EBs. (*H*) MEA recordings after propranolol (2 μM) administration in LQTS-iPSC-derived beating EBs during isoproterenol-induced VT-like arrhythmia.

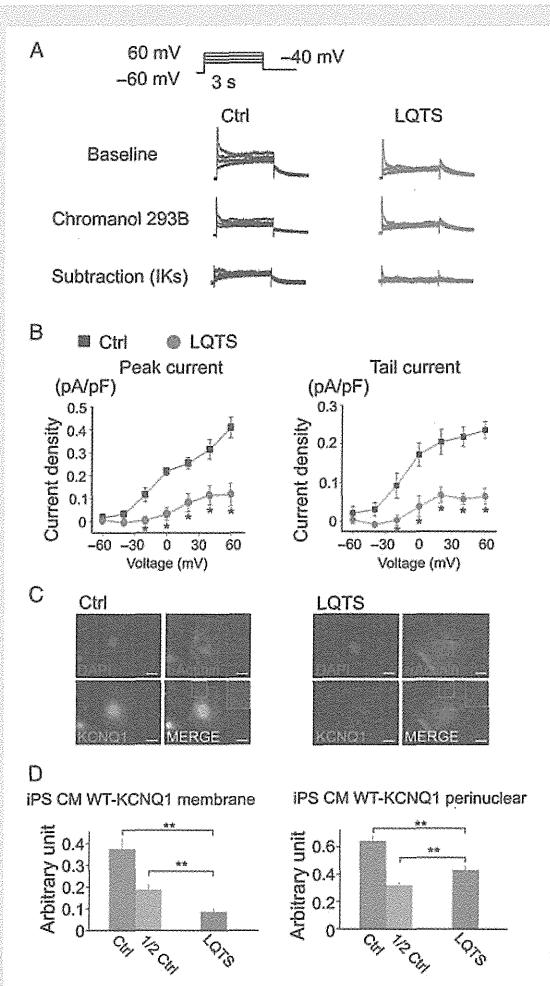


**Figure 5** Dominant-negative role of the *KCNQ1* 1893delC mutant in iPSC-derived cardiomyocytes. (*A*) The pulse protocol is shown in the upper panel. Representative current traces of baseline, chromanol 293B (30 μM) administration and subtraction expressed in control- and LQTS-iPSC-derived cardiomyocytes. (*B*) In the left panel, current–voltage relationship of peak current during the test depolarization pulse in control- and LQTS-iPSC-derived cardiomyocytes. In the right panel, current–voltage relationship of tail current upon repolarization to −40 mV following test depolarization in control- ($n = 7$) and LQTS-iPSC-derived cardiomyocytes ($n = 7$). (*C*) Immunofluorescence staining for KCNQ1 and α-Actinin staining in control- and LQTS-iPSC-derived cardiomyocytes. White boxes in each figure are shown at a higher magnification in the inset. Scale bar, 20 μm. (*D*) Densitometric analyses for WT-KCNQ1 expression at membrane peripheral and perinuclear sites in control- ($n = 20$) and LQTS-iPSC-derived cardiomyocytes (CM) ($n = 20$).

carrying 100% WT and 50% WT gene introduction showed cell peripheral expression of KCNQ1, which suggested normal shuttling of the KCNQ1 protein into the cell membrane (*Figure 6D* and *E* and Supplementary material online, *Figure S6*). In contrast, 100% MT and 50/50% WT and MT gene introduction induced KCNQ1 protein accumulation around the perinuclear cytoplasm, instead of at the cell periphery (*Figure 6D* and *E* and Supplementary material online, *Figure S6*). These data indicated that MT-KCNQ1 expression is down-regulated at the membrane peripheral site, which suggests that *KCNQ1* 1893delC has a dominant-negative effect via a trafficking deficiency.

## 4. Discussion

Human iPSCs have become a promising tool to analyse genetic diseases. Some previous reports indicated that disease-specific iPSCs recapitulated the disease phenotypes.[10–13] However, most patients for generating iPSCs in previous reports were already diagnosed with responsible genes and/or had familial history.[10–13,31,32] We showed here that iPSCs can recapitulate the phenotype of a sporadic patient with LQTS type1. We also performed functional analysis of the novel mutation by using patient-specific iPSCs, which may support the diagnosis of LQTS type 1 with novel mutation. Moreover, using this system allowed us to perform several drug administration tests on the iPSC-derived cardiomyocytes, which would be a realistic risk to such a patient in real medical practice. Patients with LQTS type 1 have to take β-blockers throughout their lives, and thus to confirm that β-blockers truly prevent arrhythmic events in the patients with novel mutations, patient-specific iPSC-derived cardiomyocytes could also be used for drug evaluation and monitoring.

We generated iPSCs from a sporadic LQTS patient with a novel heterozygous mutation located in the *KCNQ1* gene, 1893delC, and differentiated into cardiomyocytes. The electrophysiological function was measured by the MEA system, and we confirmed that cFPD was markedly prolonged in LQTS, as compared with control. Next, we tried to confirm the responsible channel for disease phenotype by precise examination of several drug responses. IKr is responsible for the main potassium current in cardiomyocytes and the IKr blocker significantly prolonged cFPD in LQTS- and control-iPSC-derived beating EBs. But interestingly, we observed more frequently the arrhythmogenic events like EAD in LQTS-derived beating EBs, and PVT-like arrhythmia findings recorded only in LQTS. In addition, IKs is another important potassium current in cardiomyocytes but the IKs blocker did not affect cFPD in LQTS, though it significantly prolonged control's cFPD in a dose-dependent manner. In general, IKr and IKs channels work in a complementary fashion in cardiomyocytes, which is known as repolarization reserve.[28,29,33] Taken together with IKr and IKs administration, we could propose that IKs channels were functionally impaired and that IKr channels would compensate for this effect in the patient-derived iPSCs. It was also supported that the diagnosis of our patient may be LQTS type1 because of the onset of the ventricular fibrillation caused by exertional stress.[20,21] It is important to elucidate whether the disease phenotype is reproducible in the same clinical situation, but it should be better to avoid reproducing ventricular fibrillation in those patients because of the high risk of sudden death. Therefore, we examined whether adrenergic stimulation can cause arrhythmogenic events in LQTS-iPSCs-derived cardiomyocytes. We successfully reproduced that the β-stimulant, isoproterenol, induced VT-like arrhythmia only in LQTS, which was totally blocked by the β-blocker, propranolol. These findings strongly suggested that patient's IKs channels were functionally impaired and we focused on the identification of the responsible gene mutation in the *KCNQ1* gene. To confirm the dominant-negative role of the *KCNQ1* 1893delC mutation in IKs channel function, we examined electrophysiological and histochemical analyses in iPSC-derived

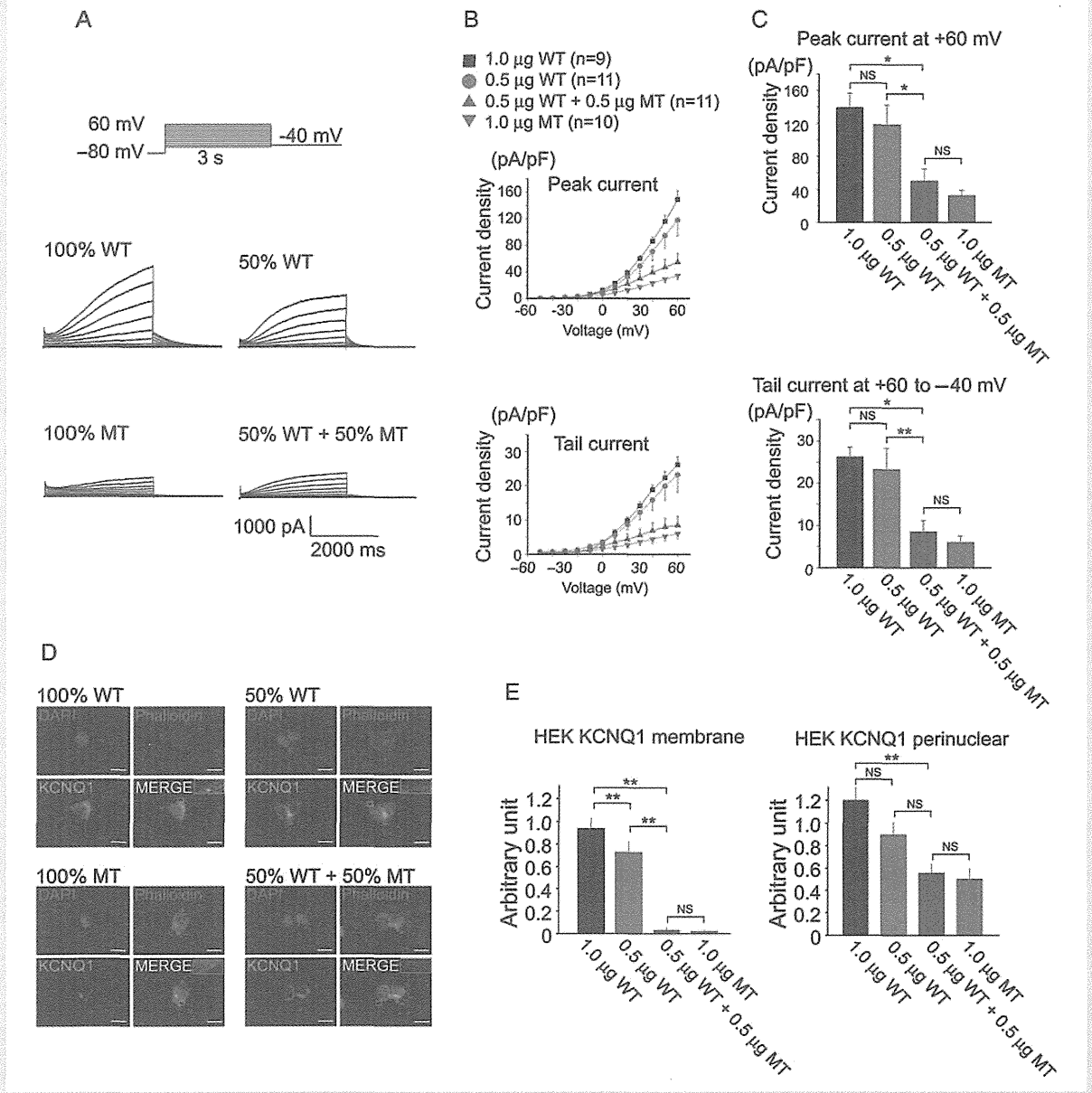


**Figure 6** Dominant-negative role of the *KCNQ1* 1893delC mutant in HEK cells. (*A*) The pulse protocol is shown in the upper left panel. Representative current traces of WT- and/or P631fs/33-KCNQ1 expressed in HEK cells. Cells of each panel were transfected as follows: 100% WT-KCNQ1, 50% WT-KCNQ1, 50% WT + 50% P631fs/33-KCNQ1, and 100% P631fs/33-KCNQ1. (*B*) In the upper panel, current–voltage relationship of peak current during the test depolarization pulse in HEK cells introduced with 100% WT, 50% WT, 100% MT, and 50% WT + 50% MT *KCNQ1* genes. In the lower panel, current–voltage relationship of tail current upon repolarization to −40 mV following test depolarization in HEK cells introduced with 100% WT, 50% WT, 100% MT, and 50% WT + 50% MT *KCNQ1* genes. (*C*) Summary of the peak and tail current densities measured following the test depolarization pulse of +60 mV. In the upper panel, bar graphs showing current densities of developing (peak) recorded current at +60 mV. In the lower panel, bar graphs showing current densities of tail current recorded upon repolarization to −40 mV from +60 mV test depolarization. (*D*) Immunofluorescence staining for KCNQ1 and phalloidin staining in HEK cells introduced with 100% WT, 50% WT, 100% MT, and 50% WT + 50% MT *KCNQ1* genes. White boxes in each figure are shown at higher magnifications in the inset. Scale bar, 20 μm. (*E*) Densitometric analyses for KCNQ1 expression at membrane peripheral and perinuclear sites in HEK cells introduced with 100% WT ($n = 14$), 50% WT ($n = 15$), 100% MT ($n = 14$), and 50% WT + 50% MT *KCNQ1* genes ($n = 13$).

cardiomyocytes, and showed that *KCNQ1* 1893delC has a dominant-negative effect via a trafficking deficiency. And there remains a possibility that other mutated genes might be involved in disease phenotypes. So we examined electrophysiological and histochemical analyses in HEK cells in which WT and MT *KCNQ1* genes were transferred, and showed that *KCNQ1* 1893delC has a dominant-negative effect via a trafficking deficiency.

This study had several limitations with respect to basic research and clinical application. In our study, the control subjects were two healthy volunteers who were unrelated to the patient. The type of such controls that are optimal to use in disease modelling using patient-specific iPSCs remains under discussion.[34] To examine pure functions of the mutated genes, it would seem better to compare patient's family members who do not harbour the mutation, although related family members share genetic information including single nucleotide polymorphisms, and this could affect disease phenotypes. A recent study also showed that ideal control iPSCs can be obtained by mutated gene correction using a targeting strategy.[35] However, it is sometimes difficult to establish iPSCs from family members and correct a mutated gene in human iPSCs. In our study, we used control iPSCs from healthy unrelated volunteers and also performed functional analysis of the mutated genes using gene transduction. Another important issue for routine clinical application of disease modelling using iPSCs is the time path. It takes a few months to generate iPSCs from the patient's dermal fibroblasts, and another few months to differentiate iPSCs into cardiac myocytes. Thus, a minimum of half of year is required to generate iPSC-derived cardiomyocytes that reproduce the patient's phenotype. Although iPSC technology is an attractive tool for analysing human diseases, it is clear that technological innovation remains necessary for the use of iPSCs in routine medical practice.

In the present study, we showed that patient-derived iPSCs could recapitulate disease phenotype in a case of sporadic LQTS. Importantly, this study demonstrated that iPSCs could be useful to characterize the electrophysiological cellular phenotype of a patient with a novel mutation. In terms of effort, cost, and time, such a method for characterizing a phenotype should overcome several problems that remain in realizing the routine clinical application potential of patient-derived iPSC technology, and in turn, the promise of personalized medicine in the future clinical setting.

## Supplementary material

Supplementary material is available at *Cardiovascular Research* online.

## Acknowledgements

The authors are grateful to Yoko Shiozawa for her technical assistance.

**Conflict of interest:** none declared.

## Funding

This study was supported in part by research grants from the Ministry of Education, Science and Culture, Japan, by the Programme for Promotion of Fundamental Studies in Health Science of the National Institute of Biomedical Innovation and Health Labour Sciences Research Grant.

## References

1. Rea TD, Page RL. Community approaches to improve resuscitation after out-of-hospital sudden cardiac arrest. *Circulation* 2010;**121**:1134–1140.
2. Zipes DP, Wellens HJJ. Sudden cardiac death. *Circulation* 1998;**98**:2334–2351.
3. Goldenberg I, Moss AJ. Long QT syndrome. *J Am Coll Cardiol* 2008;**51**:2291–2300.
4. Morita H, Wu J, Zipes DP. The QT syndromes: long and short. *Lancet* 2008;**372**: 750–763.
5. Huikuri HV, Castellanos A, Myerburg RJ. Sudden death due to cardiac arrhythmias. *N Engl J Med* 2001;**345**:1473–1482.
6. Priori SG, Napolitano C, Schwartz PJ. Low penetrance in the long-QT syndrome : clinical impact. *Circulation* 1999;**99**:529–533.
7. Bokil NJ, Baisden JM, Radford DJ, Summers KM. Molecular genetics of long QT syndrome. *Mol Genet Metab* 2010;**101**:1–8.
8. Takahashi K, Tanabe K, Ohnuki M, Narita M, Ichisaka T, Tomoda K *et al.* Induction of pluripotent stem cells from adult human fibroblasts by defined factors. *Cell* 2007;**131**: 861–872.
9. Yu J, Vodyanik MA, Smuga-Otto K, Antosiewicz-Bourget J, Frane JL, Tian S *et al.* Induced pluripotent stem cell lines derived from human somatic cells. *Science* 2007; **318**:1917–1920.
10. Moretti A, Bellin M, Welling A, Jung CB, Lam JT, Bott-Flügel L *et al.* Patient-specific induced pluripotent stem-cell models for long-QT syndrome. *N Engl J Med* 2010; **363**:1397–1409.
11. Itzhaki I, Maizels L, Huber I, Zwi-Dantsis L, Caspi O, Winterstern A *et al.* Modelling the long QT syndrome with induced pluripotent stem cells. *Nature* 2011;**471**: 225–229.
12. Yazawa M, Hsueh B, Jia X, Pasca AM, Bernstein JA, Hallmayer J *et al.* Using induced pluripotent stem cells to investigate cardiac phenotypes in Timothy syndrome. *Nature* 2011;**471**:230–234.
13. Matsa E, Rajamohan D, Dick E, Young L, Mellor I, Staniforth A *et al.* Drug evaluation in cardiomyocytes derived from human induced pluripotent stem cells carrying a long QT syndrome type 2 mutation. *Eur Heart J* 2011;**32**:952–962.
14. World medical association declaration of Helsinki: recommendations guiding physicians in biomedical research involving human subjects. *Cardiovasc Res* 1997;**35**:2–3.
15. Shimoji K, Yuasa S, Onizuka T, Hattori F, Tanaka T, Hara M *et al.* G-CSF promotes the proliferation of developing cardiomyocytes in vivo and in derivation from ESCs and iPSCs. *Cell Stem Cell* 2010;**6**:227–237.
16. Massaeli H, Guo J, Xu J, Zhang S. Extracellular K+ is a prerequisite for the function and plasma membrane stability of HERG channels. *Circ Res* 2010;**106**: 1072–1082.
17. Ravera S, Aluigi MG, Calzia D, Ramoino P, Morelli A, Panfoli I. Evidence for ectopic aerobic ATP production on C6 glioma cell plasma membrane. *Cell Mol Neurobiol* 2011;**31**:313–321.
18. Zwi L, Caspi O, Arbel G, Huber I, Gepstein A, Park I-H *et al.* Cardiomyocyte differentiation of human induced pluripotent stem cells. *Circulation* 2009;**120**: 1513–1523.
19. Zipes DP, Camm AJ, Borggrefe M, Buxton AE, Chaitman B, Fromer M *et al.* ACC/AHA/ESC 2006 Guidelines for Management of Patients With Ventricular Arrhythmias and the Prevention of Sudden Cardiac Death: A Report of the American College of Cardiology/American Heart Association Task Force and the European Society of Cardiology Committee for Practice Guidelines (writing committee to develop guidelines for management of patients with ventricular arrhythmias and the prevention of sudden cardiac death): developed in collaboration with the European Heart Rhythm Association and the Heart Rhythm Society. *Circulation* 2006;**114**: e385–484.
20. Vyas H, Hejlik J, Ackerman MJ. Epinephrine QT stress testing in the evaluation of congenital long-qt syndrome: diagnostic accuracy of the paradoxical QT response. *Circulation* 2006;**113**:1385–1392.
21. Shimizu W, Noda T, Takaki H, Nagaya N, Satomi K, Kurita T *et al.* Diagnostic value of epinephrine test for genotyping LQT1, LQT2, and LQT3 forms of congenital long QT syndrome. *Heart Rhythm* 2004;**1**:276–283.
22. Napolitano C, Priori SG, Schwartz PJ, Bloise R, Ronchetti E, Nastoli J *et al.* Genetic testing in the long QT syndrome. *JAMA* 2005;**294**:2975–2980.
23. Seki T, Yuasa S, Oda M, Egashira T, Yae K, Kusumoto D *et al.* Generation of induced pluripotent stem cells from human terminally differentiated circulating T cells. *Cell Stem Cell* 2010;**7**:11–14.
24. Sartiani L, Bettiol E, Stillitano F, Mugelli A, Cerbai E, Jaconi ME. Developmental changes in cardiomyocytes differentiated from human embryonic stem cells: a molecular and electrophysiological approach. *Stem Cells* 2007;**25**:1136–1144.
25. Jiang P, Rushing SN, Kong C-w, Fu J, Lieu DK-T, Chan CW *et al.* Electrophysiological properties of human induced pluripotent stem cells. *Am J Physiol Cell Physiol* 2010;**298**: C486–C495.
26. Tanaka T, Tohyama S, Murata M, Nomura F, Kaneko T, Chen H *et al. In vitro* pharmacologic testing using human induced pluripotent stem cell-derived cardiomyocytes. *Biochem Biophys Res Commun* 2009;**385**:497–502.
27. Marban E. Cardiac channelopathies. *Nature* 2002;**415**:213–218.
28. Roden DM, Abraham RL. Refining repolarization reserve. *Heart Rhythm* 2011;**8**: 1756–1757.
29. Jost N, Papp JG, Varró A. Slow delayed rectifier potassium current (IKs) and the repolarization reserve. *Ann Noninvas Electrocardiol* 2007;**12**:64–78.
30. Viskin S, Halkin A. Treating the long-QT syndrome in the era of implantable defibrillators. *Circulation* 2009;**119**:204–206.

31. Carvajal-Vergara X, Sevilla A, D'Souza SL, Ang Y-S, Schaniel C, Lee D-F *et al.* Patient-specific induced pluripotent stem-cell-derived models of LEOPARD syndrome. *Nature* 2010;**465**:808–812.
32. Park I-H, Arora N, Huo H, Maherali N, Ahfeldt T, Shimamura A *et al.* Disease-specific induced pluripotent stem cells. *Cell* 2008;**134**:877–886.
33. Emori T, Antzelevitch C. Cellular basis for complex T waves and arrhythmic activity following combined IKr and IKs block. *J Cardiovasc Electrophysiol* 2001;**12**:1369–1378.
34. Cheung AY, Horvath LM, Grafodatskaya D, Pasceri P, Weksberg R, Hotta A *et al.* Isolation of MECP2-null Rett syndrome patient hiPS cells and isogenic controls through X-chromosome inactivation. *Hum Mol Genet* 2011;**20**: 2103–2115.
35. Soldner F, Laganiere J, Cheng AW, Hockemeyer D, Gao Q, Alagappan R *et al.* Generation of isogenic pluripotent stem cells differing exclusively at two early onset Parkinson point mutations. *Cell* 2011;**146**:318–331.

Circulation Journal
Official Journal of the Japanese Circulation Society
http://www.j-circ.or.jp

ORIGINAL ARTICLE
Arrhythmia/Electrophysiology

# Seasonal and Circadian Distributions of Cardiac Events in Genotyped Patients With Congenital Long QT Syndrome

Masateru Takigawa, MD; Mihoko Kawamura, MD; Takashi Noda, MD, PhD; Yuko Yamada, MD; Koji Miyamoto, MD; Hideo Okamura, MD; Kazuhiro Satomi, MD, PhD; Takeshi Aiba, MD, PhD; Shiro Kamakura, MD, PhD; Tomoko Sakaguchi, MD, PhD; Yuka Mizusawa, MD; Hideki Itoh, MD, PhD; Minoru Horie, MD, PhD; Wataru Shimizu, MD, PhD

***Background:*** Although the incidence of ventricular tachyarrhythmias associated with structural heart disease is highest in winter and during the daytime, seasonal and circadian variations among cardiac events in patients with congenital long QT syndrome (LQTS) remain unknown. The present study aims to determine seasonal and circadian cardiac events in patients with a congenital LQTS genotype.

***Methods and Results:*** The medical records of 196 consecutive patients with symptomatic LQTS (age, 32±19 years; female, n=133; LQT1, n=86; LQT2, n=95; LQT3, n=15) who were genotyped between 1979 and 2006 at 2 major Japanese institutions were retrospectively analyzed. The patients with LQT1, LQT2, and LQT3 developed 223,550 and 59 cardiac events during a mean follow-up of 26, 33, and 25 years, respectively. The numbers of cardiac events significantly peaked during the summer among those with LQT1 (P<0.001) and from summer to fall in those with LQT2 (P<0.001), but reached the nadir in winter among those with LQT3 (P=0.003). Cardiac events significantly peaked in the afternoon (12:00–17:59) and morning (06:00–11:59) among those with LQT1 (P<0.001) and LQT2 (P<0.001).

***Conclusions:*** The frequency of cardiac events was specifically seasonal and circadian among patients with the 3 major genotypes of congenital LQTS. (*Circ J* 2012; **76:** 2112–2118)

**Key Words:** Cardiac events; Circadian; Long QT syndrome; Seasonal

Congenital long-QT syndrome (LQTS) is caused by mutations in genes encoding channels that regulate potassium, sodium, or calcium currents, and by mutations in a cytoskeletal gene that affects sodium and calcium kinetics, resulting in prolonged ventricular repolarization and an increased risk for sustained ventricular tachyarrhythmias.[1] Although the incidence of ventricular tachyarrhythmias including ventricular tachycardia (VT) and ventricular fibrillation (VF) is the highest in winter and during the daytime among patients with structural heart disease,[2–9] the seasonal and circadian occurrence of cardiac events as a result of torsade de pointes remains unknown in patients with congenital LQTS.

We analyzed the medical records of patients genotyped with congenital LQTS to determine the seasonal and circadian occurrence of cardiac events.

## Methods

### Study Population

The present study included 196 (age, 32±19 years; female, n=133) consecutive patients with symptomatic LQTS and detailed medical information who were genotyped at 2 major Japanese institutions (National Cerebral and Cardiovascular Center, Suita, and Shiga University of Medical Science, Ohtsu)

Received February 21, 2012; revised manuscript received April 28, 2012; accepted May 22, 2012; released online June 23, 2012 Time for primary review: 7 days

Division of Arrhythmia and Electrophysiology, Department of Cardiovascular Medicine, National Cerebral and Cardiovascular Center, Suita (M.T., T.N., Y.Y., K.M., H.O., K.S., T.A., S.K., W.S.); Department of Cardiovascular and Respiratory Medicine, Shiga University of Medical Science, Ohtsu (M.K., T.S., Y.M., H.I., M.H.), Japan

The first two authors contributed equally (M.T., M.K.).

Presented in part at the Heart Rhythm 2009, Boston, Massachusetts, USA, May 13-16, 2009, and published in abstract form (Heart Rhythm. 2009; May, S162).

Current address: Cardiovascular Center, Department of Internal Medicine, Yokosuka Kyosai Hospital, Yokosuka, Kanagawa, Japan (M.T.).

Mailing address: Wataru Shimizu, MD, PhD, Division of Arrhythmia and Electrophysiology, Department of Cardiovascular Medicine, National Cerebral and Cardiovascular Center, 5-7-1 Fujishiro-dai, Suita 565-8565, Japan. E-mail: wshimizu@hsp.ncvc.go.jp

ISSN-1346-9843 doi:10.1253/circj.CJ-12-0213

**Table 1. Baseline Characteristics of the Study Population (n=196)**

| | LQT1 | LQT2 | LQT3 | Total |
|---|---|---|---|---|
| Patients | 86 | 95 | 15 | 196 |
| Gender, female | 60 (69.8%) | 67 (70.5%) | 6 (40.0%) | 133 (67.9%) |
| Age at the study (follow-up) | 25.8±14.1 | 32.5±14.8 | 25.3±18.1 | 28.0±15.6 |
| Age at the genetic test | 15.5±15.6 | 26.9±13.9 | 18.8±13.7 | 20.6±15.2 |
| β-blockers | 59 (68.6%) | 62 (65.3%) | 6 (40.0%) | 127 (64.8%) |
| ICD therapy | 9 (10.5%) | 16 (16.8%) | 5 (33.3%) | 30 (15.3%) |
| Total cardiac events | 223 | 550 | 59 | 832 |
| Mean events number/patient | 2.6±2.7 | 5.8±11.5 | 3.9±4.9 | 4.2±8.5 |
| Median/range events | 2 (1–18) | 3 (1–75) | 2 (1–19) | 2 (1–75) |

LQT, Long QT; ICD, implantable cardioverter defibrillator.

**Table 2. Details of Cardiac Events in Each Type of LQT Syndrome**

| | Presyncope | Syncope | Cardiac arrest or death | Total cardiac events |
|---|---|---|---|---|
| LQT1 | 16 (7.2%) | 190 (85.2%) | 17 (7.6%) | 223 |
| LQT2 | 220 (40.0%) | 311 (56.5%) | 19 (3.5%) | 550 |
| LQT3 | 2 (3.4%) | 35 (59.3%) | 22 (37.3%) | 59 |

LQT, Long QT.

between 1979 and 2006. Eighty-six, 95, and 15 patients had LQT1, LQT2, and LQT3, respectively. The LQTS patients having compound mutations or other mutations except for LQT1, LQT2, and LQT3 were excluded from the analysis. Symptoms included presyncope, syncope, and cardiac arrest. Sudden dizziness, palpitation, and chest pain persisting for over 30 s without a complete loss of consciousness confirmed by electrocardiogram (ECG) recordings as being associated with ventricular tachyarrhythmias at least once were included as presyncope. Multiple events were defined as over 2 cardiac events per 24-h period. Written informed consent was obtained from each patient in this study to undergo genetic testing. The privacy of the patients was protected by the anonymization of all data.

### Data Collection

In general, the LQTS patients were first referred to our hospital or to a local outpatient clinic for evaluation and therapy, and followed up routinely every 1–3 months. After genotyping at our hospital, they attended our outpatient clinic every 1–6 months (mean, 2.2±1.1 months; median, 2 months). The follow-up period included all periods since the first presentation at our hospital or a local outpatient clinic. A detailed history was obtained at each visit and all patients were encouraged to attend the clinic whenever they experienced palpitations, chest pain, presyncope, or syncope. Patients with cardiac arrest were usually conveyed to our hospital. We obtained as complete a medical history as possible from patients and their relatives, and retrospectively analyzed these records in detail to determine the seasonal and circadian distribution of cardiac events. Some patients were followed up at other outpatient clinics even after genetic testing when they lived far from our institutions. Local physicians or pediatric cardiologists then provided detailed information taken directly from their own medical records, as well as from the patients and their families.

Seasons are defined in the present study according to the Japanese calendar as winter, December to February; spring, March to May; summer, June to August; and fall, September to November. The time of day was classified as night-time (00:00–05:59), morning (06:00–11:59), afternoon (12:00–17:59), and evening (18:00–23:59). Triggers of cardiac events were classified as exercise, emotion, and rest or sleep without arousal according to a previous report.[10]

### Statistics

Quantitative data are presented as means±SD or medians/range, and were compared using ANOVA or Kruskal-Wallis analysis. Categorical data are presented as absolute and percentage frequencies, and were analyzed using the $\chi^2$ test. The difference in the frequency of cardiac events was analyzed using the goodness-of-fit test for multinomial distribution. A value of $P<0.05$ was considered significant.

## Results

### Patient Characteristics

The baseline characteristics of the study population are shown in **Table 1**. Females comprised about 70% of the LQT1 and LQT2 groups but only 40% of the LQT3 group. The total numbers of cardiac events were 223, 550, and 59 in the LQT1, LQT2, and LQT3 groups during a mean follow-up of 26, 33, and 25 years, respectively. The numbers of events per genotype significantly differed (P=0.007), being 2.6, 5.8, and 3.9 in the LQT1, LQT2, and LQT3 groups, respectively. **Table 2** shows details of the cardiac events that occurred in each LQTS type. The frequency of more severe symptoms of cardiac events, such as syncope, cardiac arrest, and sudden death, were higher in the LQT1 and LQT3 groups than in the LQT2 group, in which such extreme symptoms accounted for 60% of the total number of events. Symptoms such as presyncope were milder in the remaining 40% of the LQT2 group.

### Seasonal and Circadian Distribution of Cardiac Events in LQT1

Among a total of 223 cardiac events, details about the season and time of occurrence for 42 (18.8%) and 55 (24.7%) events, respectively, were vague. Among 181 (81.2%) events with de-

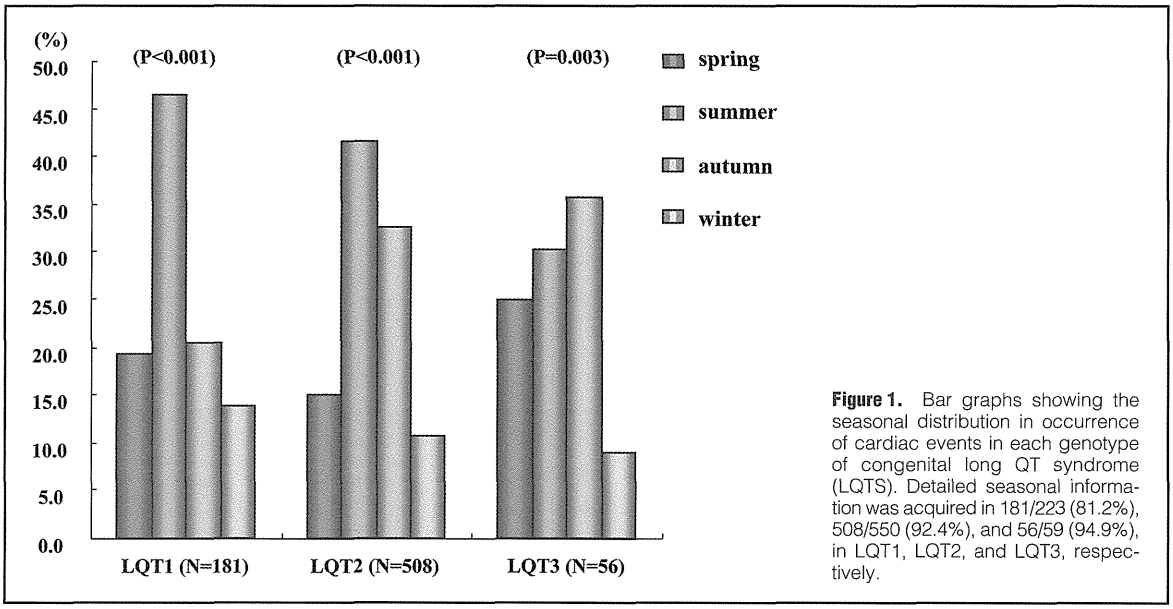


**Figure 1.** Bar graphs showing the seasonal distribution in occurrence of cardiac events in each genotype of congenital long QT syndrome (LQTS). Detailed seasonal information was acquired in 181/223 (81.2%), 508/550 (92.4%), and 56/59 (94.9%), in LQT1, LQT2, and LQT3, respectively.

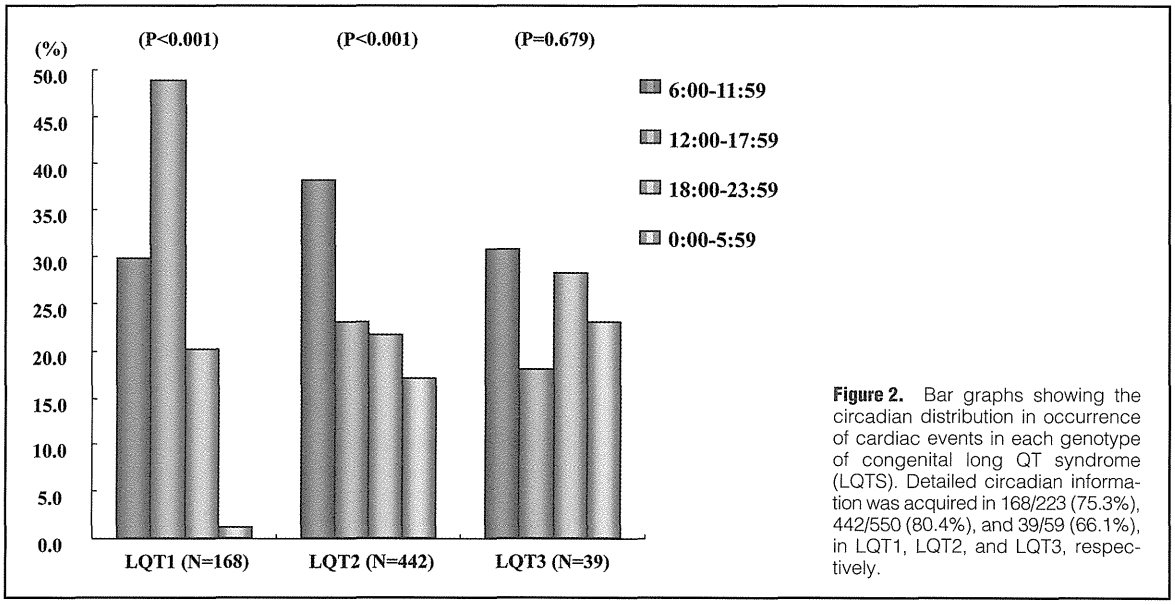


**Figure 2.** Bar graphs showing the circadian distribution in occurrence of cardiac events in each genotype of congenital long QT syndrome (LQTS). Detailed circadian information was acquired in 168/223 (75.3%), 442/550 (80.4%), and 39/59 (66.1%), in LQT1, LQT2, and LQT3, respectively.

tailed seasonal information, most occurred during the summer (84/181, 46.4%) and the frequency was lowest during the winter (25/181, 13.8%) (**Figure 1**). Among 168 (75.3%) events with detailed time information, the frequency was highest during the afternoon (82/168, 48.8%), followed by the morning (50/168, 29.8%), and lowest during the night-time (2/168, 1.2%) (**Figure 2**). Among the 50 events that occurred during the morning, extremely few arose at the time of awakening. Only 5 (10%) occurred during first 2 h of the morning (6:00–7:59) (P<0.001), and the remaining 45 (90%) events occurred during the late morning (8:00–11:59). Both the seasonal incidence of cardiac events among 3-month periods and the circadian incidence among 6-h periods statistically differed (both, P<0.001).

### Seasonal and Circadian Distribution of Cardiac Events in LQT2

Among a total of 550 cardiac events, details about the season and time of occurrence were vague for 42 (7.6%) and 108 (19.6%) events, respectively. Among 508 (92.4%) cardiac events with detailed seasonal information, the frequency was highest during the summer (211/508, 41.5%), followed by the fall (166/508, 32.7%), and lowest during the winter (55/508, 10.8%) (**Figure 1**). Among 442 (80.4%) cardiac events with

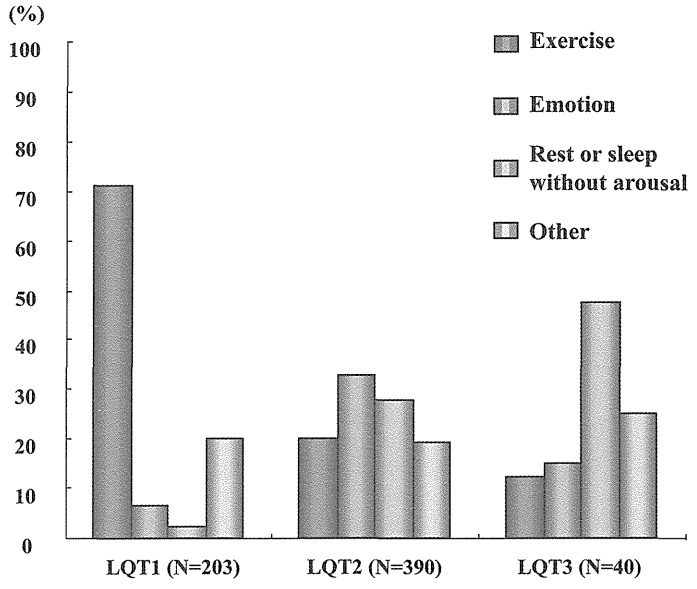


**Figure 3.** The frequency of 4 different factors triggering cardiac events are indicated as bar graphs. Detailed trigger was acquired in 203/223 (91.0%), 390/550 (70.9%), and 40/59 (67.8%), in LQT1, LQT2, and LQT3, respectively.

detailed time information, the frequency was highest during the morning (169/442, 38.2%), followed by the afternoon (102/442, 23.1%), and evening (96/442, 21.7%) (**Figure 2**), and lowest during the night-time (75/442, 17.0%) (**Figure 2**). Cardiac events associated with the morning were concentrated within the first 2h of awakening (89/169, 52.7%) between 6:00 and 7:59 (P<0.001). Both the seasonal incidence of cardiac events among the 3-month periods and the circadian incidence among the 6-h periods statistically differed (both, P<0.001).

### Seasonal and Circadian Distribution of Cardiac Events in LQT3

Among a total of 59 cardiac events, details about the season and time of occurrence were vague for 3 (5.1%) and 20 (33.9%) events, respectively. Among 56 (94.9%) events with detailed seasonal information, the frequency was the highest during the fall (20/56, 35.7%), followed by summer (17/56, 30.4%), and spring (14/56, 25.0%), and lowest during the winter (5/56, 8.9%) (**Figure 1**). Among 39 (66.1%) events with detailed time information, the frequency of cardiac events was highest at midnight in LQT3 compared with LQT1 and LQT2 (**Figure 2**). The seasonal incidence of cardiac events among the 3-month periods statistically differed (P=0.003), whereas the circadian incidence among the 6-h periods did not (P=0.679).

### Triggers of Cardiac Events in LQTS

**Figure 3** shows triggers for cardiac events. Triggers were confirmed in 203 (91.0%), 390 (70.9%), and 40 (67.8%) events in LQT1, LQT2, and LQT3, respectively. Most cardiac events in the LQT1 group developed during exercise (144/203, 70.9%), although fewer events occurred during emotional stress (13/203, 6.4%) or rest (5/203, 2.5%). Among 144 cardiac events caused by exertion, 39 (27.1%) were associated with swimming, which accounted for 52% of the triggers of cardiac events during summer exertion. No typical trigger was identified among patients with LQT2, although relatively more cardiac events developed in this group during emotional stress (128/390, 32.8%), such as arousal or being startled by the sudden ringing of a telephone or a bell, and psychological stress including fear, anxiety, and anger, and fewer developed during rest or sleep without arousal (109/390, 27.9%) or exercise (78/390, 20.0%). In addition, the features of exercise as a trigger for LQT2 were unlike those of LQT1 insofar as they were considerably milder and included routine activities such as standing from a seated position, walking, and brushing teeth. In addition, events tended to occur at the start of such activities in the LQT2 group compared with during more intense exercise in the LQT1 group. Cardiac events were more frequent during rest or sleep without arousal in the LQT3 group (19/40, 47.5%) compared with exercise (5/40, 12.5%) and emotional stress (6/40, 15.0%).

### Seasonal Distribution of Multiple Events

Multiple events occurred within 24h in 13/86 (15.1%), 30/95 (31.6%), and 4/15 (26.7%) patients with LQT1, LQT2, and LQT3, respectively. Among a total of 13 multiple events in the patients with LQT1, 2 (15.4%), 5 (38.5%), 5 (38.5%), and 1 (7.7%) occurred during the spring, summer, fall, and winter, respectively. Among a total of 55 multiple events in the LQT2 group, 3 (5.5%), 27 (49.1%), 22 (40%), and 3 (5.5%) events occurred during these respective seasons. Among a total of 4 multiple events that occurred in the LQT3 group, 2 (50.0%) occurred during the spring, 1 (25.0%) occurred during the summer, and 1 (25.0%) occurred during the winter. The seasonal distribution was significant in both the LQT1 and LQT2 groups, but was difficult to analyze in the LQT3 group because relatively few total events occurred. Over 75% and about 90% of multiple events in LQT1 and LQT2 occurred between summer and fall.

## Discussion

Although several investigators have examined the seasonal or

circadian distribution of cardiac events in patients with structural heart diseases such as old myocardial infarction,[6,9] hypertrophic cardiomyopathy,[11] idiopathic dilated cardiomyopathy,[7] or non-structural heart disease such as Brugada syndrome,[12] those associated with congenital LQT syndrome have remained unknown. We therefore examined circadian and seasonal variations in patients with LQT syndrome in multiple institutions. Our findings indicated specific seasonal and circadian distributions of cardiac events in patients with congenital LQTS that are quite different from those occurring in patients with structural heart disease. **Figure 1** shows that the incidence of cardiac events significantly peaked during the summer in LQT1 and during the summer to autumn in LQT2. Although events in LQT3 did not significantly peak during any particular season, a significant nadir was reached during the winter. Cardiac events were generally associated with more severe symptoms such as syncope, cardiac arrest, and sudden death in the LQT1 and LQT3 groups, but with milder symptoms among the LQT2 group. Triggers for cardiac events among the 3 genotypes were generally similar to those reported by others.[10,13–16] The incidence of events significantly peaked between the morning and afternoon (6:00–17:59) in LQT1, and during the morning (6:00–11:59) in LQT2 (**Figure 2**). More events occurred during the late morning in LQT1 ($P<0.001$), and around the time of awakening in LQT2 ($P<0.001$). Although a significant circadian difference was not found, the frequency of cardiac events was relatively higher during the night-time to early morning in LQT3 compared with other LQT syndromes (**Figure 3**).

### Possible Mechanisms for Seasonal Distribution of Cardiac Events

Although the frequency of cardiac events including VT/VF in patients with structural heart disease significantly increases during the winter,[2–4,17,18] the frequency was higher during summer to autumn in patients with LQT1 and LQT2 and lowest during the winter among those with LQT3. Several potential factors could explain the differences in seasonal distribution of cardiac events in patients with long QT syndrome compared with those having structural heart disease. The most likely reason for the highest frequency of cardiac events occurring in LQT1 during the summer is that participation in activities such as swimming and running is higher during the summer, and children might have more opportunities to play outside during the summer in Japan. Athletic and swimming meets are usually held during this season in schools. Sympathetic nerve activities and catecholamine levels are closely related to the occurrence of cardiac events in individuals with LQT1.[19–21] Most cardiac events occurred during exercise in our patients with LQT1, which supports previous findings.[10,13,22,23]

The reason why patients with LQT2 had the highest frequency of cardiac events from summer to early autumn remains unknown. However, seasonal variations in serum potassium levels could be 1 factor, as these levels are significantly lower in summer than in winter.[24] This could be a result of a loss of potassium through profuse sweating or increased water intake. A close correlation has been implied between hypokalemia and LQT2, in which the cell surface density of the voltage-gated $K^+$ channel, *HERG*, is regulated by a biological factor and the extracellular $K^+$ concentration, and the administration of oral potassium results in a greater reduction in resting corrected QT (QTc) interval.[25–27]

The frequency of cardiac events was lower in patients with LQT3 during the winter than during other seasons, which is similar to that of Brugada syndrome.[12] LQT3 and Brugada syndromes are both associated with mutations in SCN5A, the gene that encodes the $\alpha$ subunit of the sodium channel. Mutations in SCN5A result in an increase (gain of function) and decrease (loss of function) in the late sodium current ($I_{Na}$) in patients with LQT3 and Brugada syndrome, respectively, and are reportedly found in 18–30% of clinically diagnosed Brugada syndrome. Some single mutations in the SCN5A gene cause multiple phenotypes such as Brugada syndrome, sick sinus syndrome. and conduction disease in addition to the LQT3 phenotype.[22,28–30] In addition, recent evidence shows considerable clinical overlap, implying a new disease entity known as the overlap syndrome of cardiac sodium channelopathy.[31,32] The seasonal distribution of "multiple" events was similar to those of isolated episodes.

### Possible Mechanisms for Circadian Distribution of Cardiac Events

One factor that might explain the varied circadian distribution of cardiac events is the effect of autonomic nervous activity. Sympathetic nerve activity is higher during the daytime and upon awakening.[33–37] Cardiac events in patients with LQT1 are closely related to sympathetic nerve activities and plasma catecholamine levels, which are also higher during the daytime. In addition, daytime provides more opportunities for physical stress, because more exercise is accomplished during the daytime than during the night-time. Thus, the circadian profiles of cardiac events are similar between LQT1 and structural heart disease.

The frequency of cardiac events was significantly higher among patients with LQT2 during the early morning, when the alarm clock rings, or when they awakened, stood upright, walked, or performed daily rituals, such as face washing or brushing teeth. The response to epinephrine test in patients with LQTS reported by Noda et al might explain this circadian profile in patients with LQT2[19] in whom the QTc duration is transiently prolonged just after starting intravenous epinephrine and returns to the baseline level at the steady state. This suggests that cardiac events tend to occur immediately after an initial increase in sympathetic nerve activities or catecholamine levels, and that cardiac responses to epinephrine and or sympathetic nerve activity might be intensified at the time of awakening.

The circadian distribution of cardiac events in patients with LQT3 is difficult to conclude because of the low incidence. However, the tendency is quite similar to that of Brugada syndrome, in which cardiac events occur during the night and while asleep. Increased vagal activity apparently plays a significant role in the genesis of VF in patients with Brugada syndrome. The hereditary association in the seasonal distribution of cardiac events in LQT3 described above might participate in the coincidence of cardiac events between LQT3 and Brugada syndromes.

Darwin et al recently uncovered molecular evidence that links circadian rhythms to vulnerability in ventricular arrhythmias in mice, in which cardiac ion-channel expression and QT-interval duration (an index of myocardial repolarization) exhibit endogenous circadian rhythmicity under the control of the clock-dependent oscillator, kruppel-like factor 15 (Klf15).[38] This factor transcriptionally controls rhythmic expression of Kv channel-interacting protein 2 (KChIP2), a critical subunit required for generating the transient outward potassium current. A deficiency or excess of Klf15 causes a loss of rhythmic QT variation, abnormal repolarization, and enhanced susceptibility to ventricular arrhythmias. These mechanisms might participate in the circadian variation of ventricular arrhythmias